bioRxiv preprint doi: https://doi.org/10.1101/863894; this version posted December 4, 2019. The copyright holder for this preprint (which was not certified by peer review) is the author/funder. All rights reserved. No reuse allowed without permission.

Within-host *Mycobacterium tuberculosis* evolution: a population genetics perspective

Ana Y. Morales-Arce[*], Rebecca B. Harris[*], Anne C. Stone[*, †], & Jeffrey D. Jensen[*, ‡]

[*]Center for Evolution and Medicine, Arizona State University, Tempe, Arizona, USA
[†]School of Human Evolution and Social Change, Arizona State University, Tempe, Arizona, USA
[‡]School of Life Sciences, Arizona State University, Tempe, Arizona, USA

ABSTRACT

The within-host evolutionary dynamics of TB remain unclear, and underlying biological characteristics render standard population genetic approaches based upon the Wright-Fisher model largely inappropriate. In addition, the compact genome combined with an absence of recombination is expected to result in strong purifying selection effects. Thus, it is imperative to establish a biologically-relevant evolutionary framework incorporating these factors in order to enable an accurate study of this important human pathogen. Further, such a model is critical for inferring fundamental evolutionary parameters related to patient treatment, including mutation rates and the severity of infection bottlenecks. We here implement such a model and infer the underlying evolutionary parameters governing within-patient evolutionary dynamics. Results demonstrate that the progeny skew associated with the clonal nature of TB severely reduces genetic diversity and that the neglect of this parameter in previous studies has led to significant mis-inference of mutation rates. As such, our results suggest an underlying *de novo* mutation rate that is considerably faster than previously inferred, and a progeny distribution differing significantly from Wright-Fisher assumptions. This inference largely reconciles the seemingly contradictory observations of both rapid drug-resistance evolution but extremely low levels of genetic variation in both resistant and non-resistant populations.

bioRxiv preprint doi: https://doi.org/10.1101/863894; this version posted December 4, 2019. The copyright holder for this preprint (which was not certified by peer review) is the author/funder. All rights reserved. No reuse allowed without permission.

INTRODUCTION

Tuberculosis (TB) is a public health threat worldwide (WHO, 2018). Despite clear motivation for study, the observed within- and between-host evolutionary dynamics of *Mycobacterium tuberculosis* (*M.TB*) are not well understood, and results to date represent something of a paradox. On the one hand, drug resistance evolves rapidly (Fonseca *et al*. 2015; Eldholm *et al*. 2015); on the other, the genomic characteristics of *M.TB* do not appear conducive for such rapid adaptation, with inferred mutation rates being amongst the slowest of any human pathogen (Rocha *et al*. 2006; Ford *et al*. 2011; Ford *et al*. 2013; Colangeli *et al*. 2014; Payne *et al*. 2019; Menardo *et al.* 2019) and remarkably little genetic variation observed within or between hosts. Furthermore, purifying selection has been argued to play both a dominant as well as a weak role in shaping patterns of variation (Hershberg *et al*. 2008; Pepperell *et al*. 2013), and demographic estimates suggest a population history of TB that either matches or is uncorrelated with that of its human host (Comas *et al*. 2013; Bos *et al*. 2014; Brites *et al*. 2015; Eldholm *et al*. 2016).

To obtain a more robust understanding of TB evolutionary dynamics, it is essential to first appreciate that between-population observations are simply an aggregation of within-population processes. As such, studying the population genetics of within-patient data is critical to understanding the genetic differences observed between patients as well as their treatment outcomes. Fortunately, recent advances in sequencing technologies have allowed for more abundant and higher quality within-patient data. These published datasets have revealed a few common features of *M.TB*, including low-levels of genome-wide variation. For instance, Trauner *et al.* (2017) deep-sequenced twelve patients across four-time points and observed fewer than 50 polymorphic sites per patient genome-wide. In addition, the observed site frequency spectrum (SFS) is generally characterized by an abundance of rare variants (*i.e*., it is strongly left-skewed). These patterns have partly led to the suggestion that purifying selection effects may be wide-spread in the *M.TB* genome (Brown *et al*. 2016; Phelan *et al*. 2016; Mortimer *et al*. 2018).

Additional evolutionary factors likely contribute to these genomic patterns as well. For example, population bottlenecks may reduce genetic variation and alter the shape of the SFS (see review Thornton *et al*. 2007). Previous *M.TB* studies have investigated these effects

bioRxiv preprint doi: https://doi.org/10.1101/863894; this version posted December 4, 2019. The copyright holder for this preprint (which was not certified by peer review) is the author/funder. All rights reserved. No reuse allowed without permission.

separately in both the deep-time view of the population bottleneck and subsequent growth experienced by the host human population (Hershberg *et al*. 2008, Liu *et al*. 2018), as well as the shallow-time view of the population bottleneck and subsequent growth characterizing each novel transmission event and treatment (*e.g.,* Trauner *et al*. 2017). Additionally, in fitting the left-skewed SFS, Pepperell *et al.* (2013) found that such a demographic history combined with a mix of both deleterious and neutrally-evolving sites produced the nearest fit to the observed SFS. Finally, given the lack of recombination in *M.TB*, related linkage effects (*i.e*., background selection (Charlesworth *et al*. 1993)) have similarly been discussed within these contexts (Pepperell *et al*. 2010; Copin *et al*. 2016).

While these studies have provided many important insights, there remains a relatively unexplored, though potentially highly significant, effect: clonality. Indeed, clonality and the related progeny distribution represents an important violation of commonly used evolutionary inference approaches based upon the Wright-Fisher (WF) model and the related Kingman coalescent (Eldon *et al*. 2006; Dos Vultos *et al*. 2008; Huillet *et al*. 2011; Lapierre *et al*. 2016). Specifically, progeny distributions under the WF model are Poisson distributed with a mean and variance of 1. Therefore, when an individual produces many offspring, far in excess of simple replacement in the next generation, the assumption that only two lineages coalesce at a time is violated, resulting in multiple-merger coalescent (MMC) events (see reviews of Tellier & Lemaire 2014; Irwin *et al.* 2016).

While perhaps abstract at first blush, this violation has very important implications for the study of sequence variation and diversity. Namely, as *M.TB* has been found to exhibit strong progeny skew owing to obligate clonal reproduction (Baker *et al*. 2004; Dos Vultos *et al*. 2008), the null model against which the above studies are comparing becomes incorrect. For example, under a multiple-merger model, the effective population size (N_e) no longer scales linearly with census size (N) as it does under the Kingman coalescent (Huillet *et al*. 2011). As a result, genetic diversity is a nonlinear function of the underlying population size - a result of interest given the strongly constrained and similar levels of variation observed across TB patients, regardless of infection time or resistance status. Similarly, under these progeny-skew models, the SFS is skewed towards an excess of low-frequency variants, generating a negative Tajima's *D* even

bioRxiv preprint doi: https://doi.org/10.1101/863894; this version posted December 4, 2019. The copyright holder for this preprint (which was not certified by peer review) is the author/funder. All rights reserved. No reuse allowed without permission.

under equilibrium neutrality (Eldon *et al*. 2006; Birkner *et al*. 2013; Blath *et al*. 2016) – which appears of relevance to *M.TB* populations given the pervasively left-skewed SFS observed both within and between TB patients. Finally, the fixation probability of beneficial mutations under progeny skew may become much larger than under the WF model, owing to the increased probability of rapidly escaping stochastic loss (Der *et al*. 2011). This is fundamental to understanding the rapidly and independently evolving drug-resistance mutations in global TB populations - a result seemingly at odds with the previously inferred mutation rates (Sherman *et al*. 2011; Colangeli *et al*. 2014; Duchêne *et al*. 2016). In sum, the general theoretical expectations owing to progeny skew alone appear to qualitatively match empirical observations from *M.TB*; observations which, to date, have been attributed to alternate processes.

Recent progress has been made in utilizing these models to disentangle and even co-estimate patterns of demography, progeny skew, and selection. While there exist a variety of potential MMC models (see review of Tellier & Lemaire 2014), the so-called Ψ-coalescent has been a major focus of this literature given the straight-forward biological interpretation. Namely, the parameter Ψ represents the proportion of the next generation arising from a single parent (*e.g.,* $\Psi = 0.05$ implies that one individual contributes offspring that comprise 5% of the next generation). In addition to which, recent experimental measures from viral populations are offering real-time insights in to such progeny distributions (Vahey and Fletcher 2019). Three results are of particular importance here. First, Eldon *et al.* (2015) demonstrated that population growth may be distinguished from multiple-merger coalescent events owing to progeny-skew, given differing expectations in the SFS. Second, Matuszewski *et al.* (2018) derived analytical expectations for the SFS under a multiple merger coalescent model with changing population size and further demonstrated that these parameters can indeed be accurately inferred jointly within a likelihood framework. Finally, building upon the two above results as well as the approximate Bayesian statistical framework developed by Foll *et al.* (2014, 2015), Sackman *et al.* (2019) recently extended these results and demonstrated an ability to co-estimate progeny skew, effective population size, as well as per-site selection coefficients from time-sampled polymorphism data.

bioRxiv preprint doi: https://doi.org/10.1101/863894; this version posted December 4, 2019. The copyright holder for this preprint (which was not certified by peer review) is the author/funder. All rights reserved. No reuse allowed without permission.

Thus, a tremendous opportunity now exists to understand better the impact of mutation, genetic drift, and selection in dictating patterns of *M.TB* evolution and genomic variation under this more realistic coalescent model accounting for the underlying progeny distributions inherent to clonal reproduction. While the approximate Bayesian approach of Sackman *et al.* (2019) would appear ideal for this purpose, it is a time-sampled estimator reliant upon considerable levels of segregating variation in order to track changing allele frequencies (as is commonly observed in viral populations, for example). Thus, this approach is under-powered given the minimal levels of variation observed in *M.TB*. Further, as the underlying mutation rate itself is a question of great interest and importance in *M.TB* (Payne *et al*. 2019), it is desirable to additionally co-estimate this parameter rather than assume it to be known.

With this motivation, we developed a novel statistical approach utilizing the insights described above pertaining to infection dynamics and widespread purifying selection, while overlaying inference of underlying mutation rates, progeny distributions, and the severities of infection-related population bottlenecks. By re-analyzing published data within this framework, our results demonstrate the great importance of the multiple merger consideration and resolve many of the evolutionary paradoxes surrounding *M.TB*.

MATERIALS AND METHODS

Simulations

We conducted forward-in-time simulations using the SLIM version 3 software package (Haller & Messer 2019). *M.TB* populations were modeled using a genome size of 441,153 kb, equivalent to a tenth portion of the true genome size, for computational efficiency. As *M.TB* is a compact, highly-coding genome (Cole *et al*. 1998; Fleischmann *et al*. 2002), we assumed a distribution of fitness effects (DFE) characterized equally by deleterious (s = -0.01) and nearly neutral (s=-0.001) mutations. Mutation rate (μ) measured *in vitro* has been reported to be as slow as 2e-10 (Ford *et al*. 2011). In contrast, higher estimates ranging from 1e-9 to 9e-6 (Ford *et al*. 2013) have been proposed; therefore, our study considered the full extent of this range. Furthermore, it is important to note that previous experiments have measured only the neutral mutation rate, not the total mutation rate. In other words, the large input of strongly deleterious mutations - comprising a substantial component of the total mutation rate - has not been included

bioRxiv preprint doi: https://doi.org/10.1101/863894; this version posted December 4, 2019. The copyright holder for this preprint (which was not certified by peer review) is the author/funder. All rights reserved. No reuse allowed without permission.

in earlier estimates as these mutations are unlikely to be sampled as segregating variation or as fixed differences. However, as these mutations are important for shaping diversity via both purifying selection and background selection effects, and as our interest is in understanding the total rate at which all *de novo* mutations are input into the population, we considered the total rather than the neutral mutation rate. In order to infer this parameter within the context of an appropriate progeny-skew model, μ was drawn from a prior uniform distribution between 1e-9 and 9e-6 per site per generation.

Following an initial burn-in period of 10N generations, we considered a three-stage demographic model characterizing a single patient infection: moving forward in time, we describe 1) a neutral equilibrium population of size N, 2) an initial infection bottleneck leading to an instantaneous population reduction to size $N2$, and 3) a subsequent population size recovery to size N. In stage 1, we modeled a population of size N = 1,000. In order to quantify the effects of underlying assumptions pertaining to population size, additional simulations and inference were performed at N = 25,000. During stage 2, the severity of the population bottleneck (β) was sampled from ~U[0.001, 0.1], where $N2 = N*\beta$ - as the distribution of infection size in humans is unknown. However, it has been reported that in cattle TB (*M. bovis*) infection can be established by a single cell forming unit (Dean *et al*. 2005). During stage 2, the degree of progeny skew (or Ψ) was sampled from a prior distribution of ~U[0, 0.2]. A value of 0 corresponds to the standard WF model. Progeny skew was simulated following the procedure of Sackman *et al.* 2019. In brief, one individual is chosen from the primary population A and founds a separate subpopulation B, the single generation unidirectional migration rate from B to A is set to Ψ, and the chosen individual thus contributes $N\Psi$ offspring to the following generation of A. A series of mate choice callbacks in SLiM force the migration rate to be exact rather than stochastic (see Supplementary Materials of Sackman *et al*. 2019). Subpopulation B is removed, the next generation begins, and a new individual is randomly sampled for the following generation. As such, each generation is a combination of $N(1- \Psi)$ replacement events and a single sweepstakes event of magnitude $N\Psi$. To emulate patient sampling at the onset of symptoms (approximately three months minimum (Behr *et al*. 2018)), we allowed stage 2 to run for 90 generations, assuming a generation time of 24 hours (Cole *et al*. 1998), and stage 3 to run for 910

bioRxiv preprint doi: https://doi.org/10.1101/863894; this version posted December 4, 2019. The copyright holder for this preprint (which was not certified by peer review) is the author/funder. All rights reserved. No reuse allowed without permission.

generations before outputting genome alignments in ms format. Thus, the total generation time of our model was 11*N*.

Drawing from these prior distributions, 10,000 points (*i.e.,* parameter combinations) were sampled. For each parameter combination, we conducted 1,000 replicates in order to characterize both the mean and variance. Summary statistics were calculated in the R package PopGenome version 2.6.1 (Pfeifer *et al*. 2014).

Data analysis and joint posterior estimates

For comparison to patient data, we examined the distribution and mean of segregating sites in samples published by Trauner *et al*. (2017). (https://zenodo.org/record/322377#.XO2CAy2ZNBw). A subset of 1,000 populations was simulated under the conditions described above. Given that patient data are subject to stringent filtering criteria, removing SNPs under a particular frequency cut-off, it was necessary to filter the simulated data to allow fair comparison. Thus, 100 genomes were sampled per each simulated population, and variants < 2% frequency were filtered out before the calculation of summary statistics (Table S1). Afterward, only genomes with ≥ 2 segregating sites were considered for further analyses, and the fraction of "invariable genomes" was noted for comparison to patient samples (Figure 2 and Table S1).

RESULTS & DISCUSSION

Considering levels of variation

We here report the first joint consideration of mutation rate, purifying selection, infection history, and progeny-skew in *M.TB* populations. A correlation of summary statistics (Figure 1) demonstrates that while mutation rate (μ) increases the number of segregating sites as expected, progeny skew (Ψ) acts to reduce variation. Furthermore, as the Ψ-parameter is of relevance every generation (*i.e*., every reproduction event), the impact of this previously unconsidered progeny skew on levels of variation is in fact much stronger than the single bottleneck event associated with infection. Considering the full distribution of sampled μ values (Figure S1), it is apparent that Ψ drastically reduces the average proportion of segregating sites genome-wide even for fast

bioRxiv preprint doi: https://doi.org/10.1101/863894; this version posted December 4, 2019. The copyright holder for this preprint (which was not certified by peer review) is the author/funder. All rights reserved. No reuse allowed without permission.

mutation rates, and that the probability of producing genomes devoid of any variation will naturally increase as μ decreases.

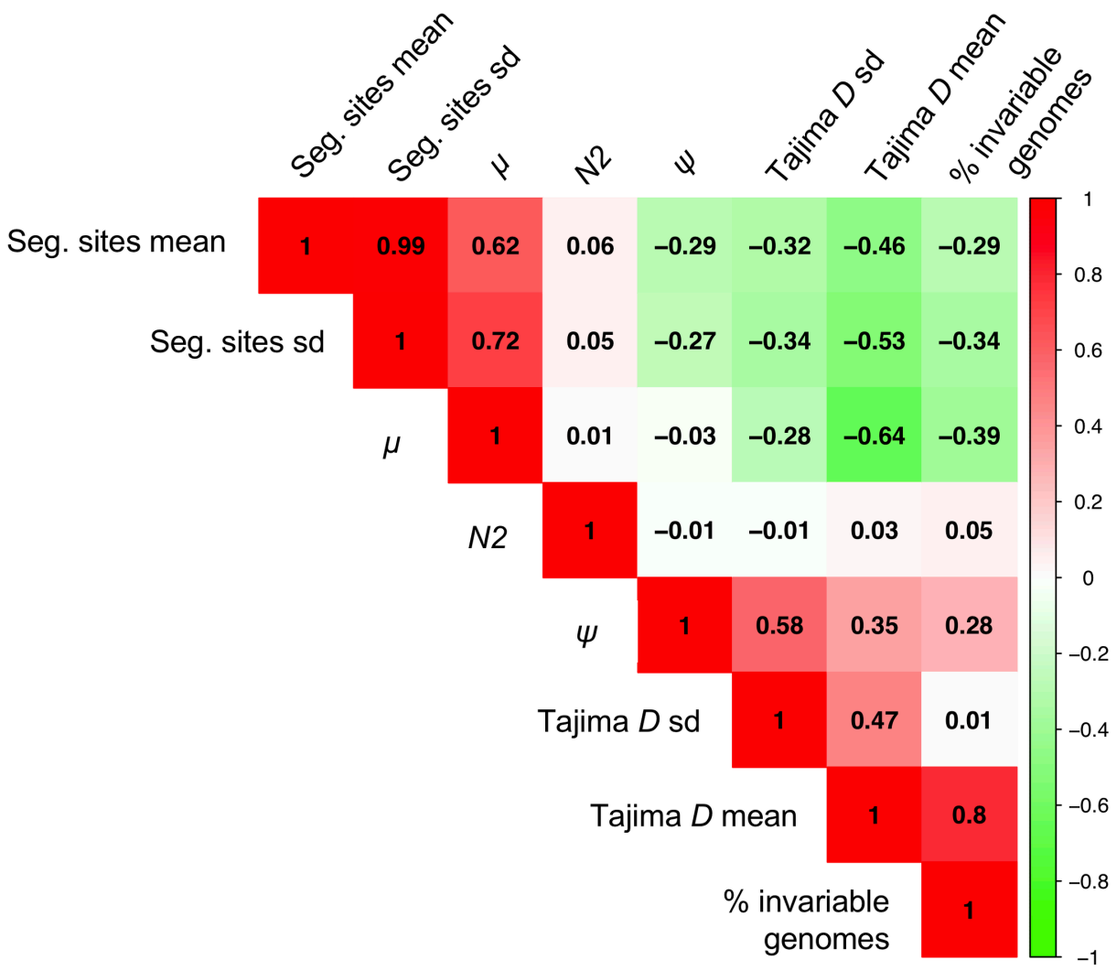


Figure 1. Correlation heatmap of parameters and summary statistics. Correlations are given between the parameters of interest (mutation rate (μ), progeny skew (Ψ), and bottleneck severity (*N2*)), and summary statistics (the mean and variance of the level of variation as measured by the number of segregating sites, and the mean and variance of the distribution of variation as measured by Tajima's *D*). As shown, *N2* values do not correlate with any of the summary statistics, as the effect of the single generation bottleneck is swamped by the per-generation reproductive skew. Further, as expected, values of μ positively correlate with the number of segregating sites, while Ψ acts to reduce variation and is thus negatively correlated. Finally, while μ would not be expected to strongly correlate with the shape of the SFS (here summarized by Tajima's *D*) for neutral mutations, it does so here given that we explicitly account for the input of deleterious mutations (see Methods).

bioRxiv preprint doi: https://doi.org/10.1101/863894; this version posted December 4, 2019. The copyright holder for this preprint (which was not certified by peer review) is the author/funder. All rights reserved. No reuse allowed without permission.

In order to consider a range of μ consistent with observed data - once pervasive purifying selection and progeny skew have been taken in to account - two examples of patient data collected by Trauner *et al.* (2017) representing low (20 segregating sites genome-wide) and high (50 segregating sites genome-wide) variation samples were plotted and compared to the simulated data. In order to compare simulated data with patient data, the same filtering steps must be applied. In this case, SNPs under 2% frequency were filtered in the empirical data, and thus, the simulated data were similarly filtered in order to be comparable (Figure 2).

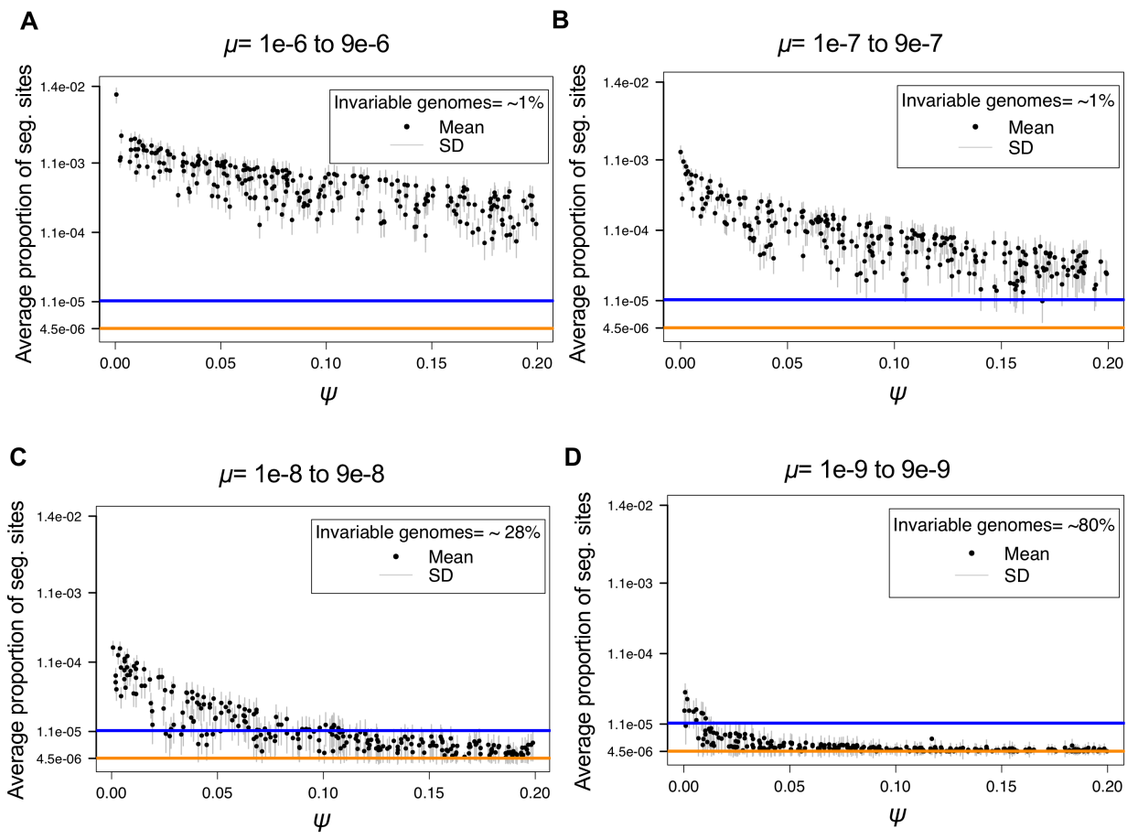


Figure 2. Log scale distribution of segregating sites above 2% frequency, as a function of mutation rate (μ) and progeny skew (Ψ). For each parameter combination (1,000 in total) of μ and Ψ drawn from the prior distributions, 1,000 replicates were simulated, with the mean given by the black dot and the standard deviation given by the gray bars. Each panel corresponds to a different order of magnitude of mutation rate range: (A) 1e-6 to 9e-6, (B) 1e-7 to 9e-7, (C) 1e-8 to 9e-8, and (D) 1e-9 to 9e-9. The colored lines correspond to two examples of the proportion of segregating sites observed genome-wide in empirical patient data: 20 segregating sites as a mean (orange), and 50 segregating sites from patient_10 (blue) (Trauner *et al.* 2017). As shown, the range of segregating sites for the fast mutation rates (panels A and B), result in expectations much larger than that observed in patient data, regardless of Ψ. Conversely, the slowest mutation rate (panel D), result in too little variation, except under WF conditions (*i.e.*, Ψ near 0) which are

bioRxiv preprint doi: https://doi.org/10.1101/863894; this version posted December 4, 2019. The copyright holder for this preprint (which was not certified by peer review) is the author/funder. All rights reserved. No reuse allowed without permission.

known to be violated given clonality. Thus, rates on the order of 1e-8 to 9e-8 (panel C) appear to well explain the range of variation observed in patient data, and further imply values of Ψ ranging roughly from 0.05 to 0.1, consistent with values previously estimated for within-host virus data (Sackman *et al*. 2019).

As shown, fast mutation rates (μ on the order of 1e-6 and 1e-7) routinely produce expected numbers of segregating sites far above that observed in patients, regardless of other parameter values, while slow mutation rates (μ on the order of 1e-9) generally result in too little variation to match observation. This result is of interest as *M.TB* mutation rates are generally believed to be exceedingly slow (Sherman *et al*. 2011) - though importantly, this inference has largely neglected the important contribution of these additional evolutionary processes. Thus, once accounting for the diversity-reducing effects inherent to clonality, as well as the extent of purifying selection effects inherent to a compact, non-recombining genome, it is evident that the *de novo* mutation rate is likely faster than previously believed, with mutation rates on the order 1e-8 well matching the range of observed data (Figure 2). In addition, in order to consider the impact of underlying assumptions pertaining to population size, simulations were re-performed with a 25x larger population size. As shown in Figure S2, owing to these diversity reducing effects, mutations rates on the order of 1e-8 remain the best fit to observed levels of variation, with slower mutation rates still producing too little variation and too many invariable genomes to be consistent with patient data.

Considering distributions of variation

For the general range of μ identified above, the number of genome-wide segregating sites in simulated population data ranged from a minimum average of 2.1 to a maximum average of 78.7 SNPs (Table S1), depending on the combination of μ and Ψ drawn from the priors. Specifically, higher values of μ may be off-set by higher values of Ψ, resulting in a similar number of segregating sites for multiple parameter combinations. For example, for the patient sample containing 10 SNPs, simulation results demonstrate that μ = 8.13e-08 and a Ψ =0.06 would produce an average of 10.15 +/-4.64 SNPs, potentially suggesting a good fit to the data. However, μ = 3.1e-08 and a Ψ =0.02 can also generate similar results, yielding 10.40 +/- 4.45 SNPs. More generally, this ridge in the posterior distributions (Figure 3A) between these two

bioRxiv preprint doi: https://doi.org/10.1101/863894; this version posted December 4, 2019. The copyright holder for this preprint (which was not certified by peer review) is the author/funder. All rights reserved. No reuse allowed without permission.

parameters suggests that they will be difficult to estimate independently if only levels of variation are used.

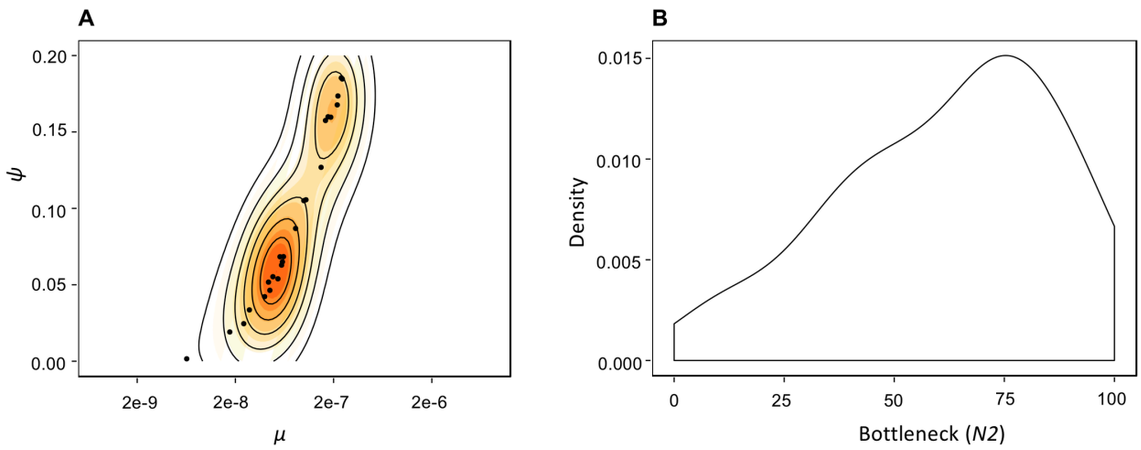


Figure 3. Posterior parameter estimates pertaining to patient data. (A) Joint posterior distribution for the parameters μ and Ψ. Solid contour lines specify the highest posterior density intervals. Owing to the diversity-increasing effect of μ and diversity-decreasing effect of Ψ, there exists a ridge in the joint posterior. Regardless, owing to differing expectations in the SFS along this ridge, inference suggests μ values within the 1e-8 range in combination with $\Psi < 0.10$. (B) Posterior density for the severity of the infection bottleneck (*N2*). The X-axis gives the number of genomes at the time of infection reduced from 1,000. While the posterior distribution is non-uniform, the observation that all tested values remain consistent with patient data strongly suggests that there is not sufficient information in the data to estimate this third parameter (*i.e.,* size of the bottleneck, in addition to μ and Ψ).

Thus, while comparisons with general levels of variation are useful for identifying a range as in the above section, more information is needed to parse values further. Importantly, previous theoretical results (Eldon & Wakeley 2016; Matuszewski *et al*. 2018) have well described the effect of Ψ on the observed distribution of genetic variation (*i.e*., SFS). To utilize this information, a general summary of the SFS, Tajima's *D* (1989), was calculated on the filtered simulated data. As shown (Figure S3), the shape of the SFS, and thus the value of the *D*-statistic, is related to the value of Ψ. As the degree of progeny skew initially increases, *D* becomes increasingly negative, as previously described. However, as progeny distributions become highly skewed, levels of variation are sharply reduced, resulting in an apparent increase in *D* values (Figure S3). Increasing *D* values could also be a result of the underlying filtering criteria, as after filtering simulations to match real data with segregating sites > 2%, *D* values

bioRxiv preprint doi: https://doi.org/10.1101/863894; this version posted December 4, 2019. The copyright holder for this preprint (which was not certified by peer review) is the author/funder. All rights reserved. No reuse allowed without permission.

increased proportionally (Figure S4). However, Tajima's *D* is consistently negative in all mutation ranges, even after filtering.

Parameter inference from patient samples

Thus, we next considered these results in light of published patient data. Recent publications have suggested that NGS technologies could facilitate personalized treatment in TB patients, allowing for improved outcomes (Copin *et al*. 2016; Cancino-Muñoz *et al*. 2019). To utilize such data, however, it is vital to understand the evolutionary dynamics shaping within-host *M.TB* diversity. As an illustrative example, we have re-examined the number of segregating sites in patient samples and estimated a mean ~10 segregating sites per sample (Trauner *et al*. 2017) (Figure S5). Further, using the results and expectations obtained above regarding the level and distribution of variation, the patient data appear best fit by simulated populations with μ values ranging from 7.3e-9 to 3.8e-7, with the strongest posterior density at $\mu \sim$ 6e-8 and $\Psi \sim$ 0.06 (Figure 3A). Notably, faster μ values could produce similar results, but only if Ψ proportions are in excess of 0.15 (Figure 3A).

In addition, owing to the strong per-generation reductions associated with progeny skew, there remains no signal in the data to estimate the severity of the infection bottleneck accurately (Figure 3B). Specifically, while there is an increase in density towards stronger bottleneck values, the posterior distribution is not notably distinct from the prior distribution ~U[0.001, 0.1] (Figure 3B). Apart from the population size reduction associated with infection, these results have important implications for the ability to detect other parameters of clinical interest - namely, the presence of selective sweeps associated with beneficial mutations (*e.g.,* potentially owing to drug-resistance). First, while there is strong statistical power to infer both μ and Ψ from patient data, there is little power to detect isolated events in the past (Figure 3B). This result, though unexpected under standard WF assumptions, is intuitive given the non-WF progeny distributions related to clonality. Namely, the diversity reduction associated with a single bottleneck event multiple generations in the past is not discernible from the per-generation diversity reduction related to clonal reproduction. Further, given that a selective sweep is, in fact, a type of population bottleneck (Barton 1998), this result also demonstrates that detecting selective sweeps associated with resistance mutations in this non-recombining organism, based

bioRxiv preprint doi: https://doi.org/10.1101/863894; this version posted December 4, 2019. The copyright holder for this preprint (which was not certified by peer review) is the author/funder. All rights reserved. No reuse allowed without permission.

on levels and patterns of genomic variation, will be exceedingly difficult. However, this observation well reconciles the fact that levels of variation do not appear significantly different between resistant and non-resistant *M.TB* patient populations (Trauner *et al*. 2017) - that is, these additional evolutionary processes are shaping variation so strongly, that the presence or absence of a resistance-associated selective sweep does not result in strongly differentiable expectations.

Implications for characterizing the history of TB in humans

A topic of wide-spread interest in the literature pertains to the history of TB in the human host. This inference has primarily been made within a phylogenetic context, relying on the construction of a single consensus sequence per patient. While such a comparison of consensus sequences can be highly mis-leading when making evolutionary inference (see Renzette *et al*. 2017), these age-estimates also inherently rely on an accurate knowledge of mutation rates in order to invoke the 'clock-like' accumulation of neutral mutations as a proxy for time (Menardo *et al.* 2019). As our results demonstrate that previous mutation rate estimates have likely been downwardly-biased, it is of interest to consider what these revised mutation rates would imply for this evolutionary history. However, there are at least three difficulties in directly comparing population-level estimates with previous consensus-based phylogenetic inference. Firstly, estimates are generally given per year, whereas the preferred evolutionary rate is per generation (as given here). There is support for one generation per day as a conversion (Cole *et al*. 1998), though further study is necessary to quantify the correct scaling factor. Secondly, when invoking a divergence-based clock, previous studies are measuring the neutral mutation rate, given that the rate of mutation is equivalent to the rate of divergence for neutral mutations only (Kimura 1968). However, we are here interested in the total mutation rate (that is, the rate at which neutral and non-neutral mutations arise per generation); therefore, our rate must be parsed into neutral and non-neutral components to enable appropriate comparison. Similar to the first point, additional research is necessary in order to better quantify the distribution of fitness effects in *M.TB,* as understanding the fraction of total mutations represented by neutral mutations is necessary for the conversion. Finally, we here consider the alleles segregating within a population for inference (*i.e.,* within a patient), whereas previous studies often call a consensus sequence per patient (*i.e.,* per population) and make inferences based on a collection of such consensus sequences. Such a summary of population-level variation into a single sequence is difficult to

bioRxiv preprint doi: https://doi.org/10.1101/863894; this version posted December 4, 2019. The copyright holder for this preprint (which was not certified by peer review) is the author/funder. All rights reserved. No reuse allowed without permission.

interpret, though what is evident is that a great majority of rare alleles will be neglected, and thus only a small subset of total variation (*i.e.,* common alleles) will be considered (Renzette *et al*. 2017). As such, we propose that future evolutionary inference pertaining to TB would benefit tremendously from a full consideration of within-patient diversity, as we demonstrate here. In sum, any direct comparison with consensus-based phylogenetic age estimates would be overly speculative at this juncture.

CONCLUSIONS

TB patient infection dynamics have remained enigmatic. We here argue that much of the difficulty in interpreting patterns of variation and evolution has owed to an inappropriate underlying null model, relying on classical expectations developed for organisms with very different underlying biological properties. Fortunately, recent theoretical extensions in non-WF and alternative coalescent models, more appropriate for clonally reproducing organisms, have created an opportunity to revisit existing *M.TB* patient data. By accounting for the pervasive purifying selection effects associated with this non-recombining, highly-coding genome, as well as the skewed progeny distributions inherent to clonal reproduction, we have provided improved insights into the evolutionary dynamics shaping within-host variation. Further, through a consideration of these diversity-reducing effects, results suggest an underlying *de novo* mutation rate that is considerably faster than previously inferred. This largely reconciles the seemingly contradictory observations of both rapid resistance evolution, but extremely low levels of population variation. Namely, the population mutation rate may indeed be sufficiently fast to provide a steady input of beneficial mutations, explaining the rapid resistance evolution clinically observed. However, recurrent purifying selection and progeny skew act together to rapidly eliminate segregating variation from the population, reconciling the minimal levels of variation observed as well as the general homogeneity in levels and distributions of variation in both resistant and non-resistant patient samples alike. Furthermore, the role of these per-generation evolutionary forces in shaping patterns of variation is sufficiently strong that periodic events, including the infection-associated bottleneck and selective sweeps centered on drug-resistance mutations, will be challenging to detect and quantify on top of these more common processes.

bioRxiv preprint doi: https://doi.org/10.1101/863894; this version posted December 4, 2019. The copyright holder for this preprint (which was not certified by peer review) is the author/funder. All rights reserved. No reuse allowed without permission.

401 **LITERATURE CITED**

402 Baker, L., T. Brown, M. C. Maiden, and F. Drobniewski. 2004. Silent nucleotide polymorphisms
403 and a phylogeny for *Mycobacterium tuberculosis*. Emerg Infect Dis. 10: 1568–1577.
404
405 Barton, N. H. 1998. The effect of hitch-hiking on neutral genealogies. Genet Res Camb.72(2):
406 123–33.
407
408 Behr, M. A., P. H. Edelstein, and L. Ramakrishnan. 2018. Revisiting the timetable of
409 tuberculosis. BMJ. 362: k2738.
410
411 Birkner, M., J. Blath, and B. Eldon. 2013. Statistical properties of the site-frequency spectrum
412 associated with Λ-coalescents. Genetics. 195: 1037–53.
413
414 Blath, J., M. Cronjäger Christensen, B. Eldon, and M. Hammer. 2016. The site-frequency
415 spectrum associated with Ξ-coalescents. Theor Popul Biol. 110: 36–50.
416
417 Bos, K. I., K. M. Harkins, A. Herbig, M. Coscolla, N. Weber *et al*. 2014. Pre-Columbian
418 mycobacterial genomes reveal seals as a source of New World human tuberculosis. Nature. 514:
419 494-497.
420
421 Brites, D., and S. Gagneux. 2015. Co-evolution of *Mycobacterium tuberculosis* and *Homo*
422 *sapiens*. Immunol Rev. 264: 6-24.
423
424 Brown, T. S., A. Narechania, J. R. Walker, P. J. Planet, P. J. Bifani, *et al.* 2016. Genomic
425 epidemiology of Lineage 4 *Mycobacterium tuberculosis* subpopulations in New York city and
426 New Jersey, 1999-2009. BMC Genomics. 17: 947.
427
428 Cancino-Muñoz, I., M. Moreno-Molina, V. Furió, G. A. Goig, M. Torres-Puente, *et al*. 2019.
429 Cryptic resistance mutations associated with misdiagnoses of multidrug-resistant tuberculosis. J
430 Infect Dis. 220: 316-320.
431
432 Charlesworth, B., M. T. Morgan, and D. Charlesworth. 1993. The effect of deleterious mutations
433 on neutral molecular variation. Genetics. 134: 1289-1303.
434
435 Colangeli, R., V. L. Arcus, R.T. Cursons, A. Ruthe, N. Karalus, *et al*. 2014. Whole genome
436 sequencing of *Mycobacterium tuberculosis* reveals slow growth and low mutation rates during
437 latent infections in humans. PLoS One. 9: 1–9.
438
439 Cole, S. T., R. Brosch, J. Parkhill, T. Garnier, C. Churcher, *et al*. 1998. Deciphering the biology
440 of *Mycobacterium tuberculosis* from the complete genome sequence. Nature. 393: 537-544.
441
442 Comas, I., M. Coscolla, T. Luo, S. Borrell, K. E. Holt, *et al*. 2013. Out-of-Africa migration and
443 Neolithic coexpansion of Mycobacterium tuberculosis with modern humans. Nat Genet.
444 45:1176–1182.
445
446 Copin, R., X. Wang, E. Louie, V. Escuyer, M. Coscolla *et al*. 2016. Within host evolution selects
447 for a dominant genotype of *Mycobacterium tuberculosis* while T cells increase pathogen genetic
448 diversity. PLoS Pathog. 12: e1006111.
449
450 Dean, G. S., S. G. Rhodes, M. Coad, A. O. Whelan, P. J. Cockle, *et al*. 2005. Minimum effective
451 dose of *Mycobacterium bovis* in cattle. Infect Immunity. 73: 6467–6471.
452
453 Der, R., C. L. Epstein, and J. B. Plotkin. 2011. Generalized population models and the nature of
454 genetic drift. Theor Popul Biol. 80: 80–99.
455
456 Dos Vultos, T., O. Mestre, J. Rauzier, M. Golec, N. Rastogi, *et al*. 2008. Evolution and diversity
457 of clonal bacteria: The paradigm of *Mycobacterium tuberculosis*. PLoS One. 3: e1538.
458
459 Duchêne, S., K. E. Holt, F. X. Weill, S. Le Hello, J. Hawkey, *et al*. 2016. Genome-scale rates of
460 evolutionary change in bacteria. Microb Genomics. 2: 1–12.
461

bioRxiv preprint doi: https://doi.org/10.1101/863894; this version posted December 4, 2019. The copyright holder for this preprint (which was not certified by peer review) is the author/funder. All rights reserved. No reuse allowed without permission.

462 Eldon, B., and J. Wakeley. 2006. Coalescent processes when the distribution of offspring number
463 among individuals is highly skewed. Genetics. 172: 2621–33.
464
465 Eldon, B., M. Birkner, J. Blath, and F. Freund. 2015. Can the site-frequency spectrum distinguish
466 exponential population growth from multiple-merger coalescents? Genetics. 199: 841–56.
467
468 Eldholm, V., J. Monteserin, A. Rieux, B. Lopez, B. Sobkowiak, *et al*. 2015. Four decades of
469 transmission of a multidrug-resistant *Mycobacterium tuberculosis* outbreak strain. Nat Commun.
470 6: 1–9.
471
472 Eldholm, V., J. H. O. Pettersson, O. B. Brynildsrud, A. Kitchen, E.M. Rasmussen, *et al*. 2016.
473 Armed conflict and population displacement as drivers of the evolution and dispersal of
474 *Mycobacterium tuberculosis*. Proc Natl Acad Sci U S A. 113:13881–6.
475
476 Fleischmann, R. D., D. Alland, J. A. Eisen, L. Carpenter, O. White, *et al*. 2002. Whole-Genome
477 comparison of *Mycobacterium tuberculosis* clinical and laboratory strains. J Bacteriol. 184:
478 5479–5490.
479
480 Foll, M., Y. P. Poh, N. Renzette, A. Ferrer-Admetlla, C. Bank, *et al*. 2014. Influenza virus drug
481 resistance: a time-sampled population genetics perspective. PLoS Genet. 10: e1004185.
482
483 Foll, M., H. Shim, and J. D. Jensen. 2015. WFABC: A Wright-Fisher ABC-based approach for
484 inferring effective population sizes and selection coefficients from time-sampled data. Mol Ecol
485 Resour. 15(1): 87–98.
486
487 Fonseca, J. D., G.M. Knight, and T. D. McHugh. 2015. The complex evolution of antibiotic
488 resistance in *Mycobacterium tuberculosis*. Int J Infect Dis. 32: 94–100.
489
490 Ford, C.B., P. L Lin, M. Chase, R.R. Shah, O. Iartchouk, *et al*. 2011. Use of whole genome
491 sequencing to estimate the mutation rate of *Mycobacterium tuberculosis* during latent infection.
492 Nat Genet. 43(5): 482-486.
493
494 Ford, C. B., R.R. Shah, M. Kato-Maeda, S. Gagneux, M. B. Murray *et al*. 2013. *Mycobacterium*
495 *tuberculosis* mutation rate estimates from different lineages predict substantial differences in the
496 emergence of drug-resistant tuberculosis. Nat Genet. 45: 784–790.
497
498 Haller, B. C., and P.W. Messer. 2019. SLiM 3: Forward genetic simulations beyond the Wright–
499 Fisher model. Mol Biol Evol. 36: 632–637.
500
501 Hershberg, R., M. Lipatov, P. M. Small, H. Sheffer, S. Niemann *et al*. 2008. High functional
502 diversity in *Mycobacterium tuberculosis* driven by genetic drift and human demography. PLoS
503 Biol. 6: e311.
504
505 Huillet, T., and M. Möhle. 2011. Population genetics models with skewed fertilities: A forward
506 and backward analysis. Stoch Model. 27: 521-554.
507
508 Irwin, K. K., S. Laurent, S. Matuszewski, S. Vuilleumier, L. Ormond, *et al*. 2016. On the
509 importance of skewed offspring distributions and background selection in virus population
510 genetics. Heredity. 117: 393–399.
511
512 Kimura, M. 1968. Evolutionary rate at the molecular level. Nature. 217: 624–626.
513
514 Lapierre, M., C. Blin, A. Lambert, G. Achaz, and E. P. C. Rocha. 2016. The impact of selection,
515 gene conversion, and biased sampling on the assessment of microbial demography. Mol Biol
516 Evol. 33: 1711–1725.
517
518 Liu, Q., A. Ma, L. Wei, Y. Pang, B. Wu, *et al*. 2018. China's tuberculosis epidemic stems from
519 historical expansion of four strains of *Mycobacterium tuberculosis*. Nat Ecol Evol. 2: 1982-1992.
520
521 Matuszewski, S., M. E. Hildebrandt, G. Achaz, and J. D. Jensen. 2018. Coalescent processes
522 with skewed offspring distributions and nonequilibrium demography. Genetics. 208: 323-338.
523

bioRxiv preprint doi: https://doi.org/10.1101/863894; this version posted December 4, 2019. The copyright holder for this preprint (which was not certified by peer review) is the author/funder. All rights reserved. No reuse allowed without permission.

524 Menardo, F., S. Duchêne, D. Brites, and S. Gagneux. 2019. The molecular clock of
525 *Mycobacterium tuberculosis.* PLoS Pathog. 15: e1008067.
526
527 Mortimer, T. D., A. M. Weber, and C. S. Pepperell. 2018. Signatures of selection at drug
528 resistance loci in *Mycobacterium tuberculosis*. mSystems. 3: e00108-17.
529
530 Payne, J. L., F. Menardo, A. Trauner, S. Borrell, S.M. Gygli, *et al*. 2019. Transition bias
531 influences the evolution of antibiotic resistance in *Mycobacterium tuberculosis*. PLOS Biol. 17:
532 e3000265.
533
534 Pepperell, C. S., V. H. Hoeppner, M. Lipatov, W. Wobeser, G. K. Schoolnik, and M. W.
535 Feldman. 2010. Bacterial genetic signatures of human social phenomena among *M. tuberculosis*
536 from an aboriginal Canadian population. Mol Biol Evol. 27: 427–40.
537
538 Pepperell, C. S., A. M. Casto, A. Kitchen, J.M. Granka, O. E. Cornejo, *et al*. 2013. The role of
539 selection in shaping diversity of natural *M. tuberculosis* populations. PLoS Pathog. 9: e1003543.
540
541 Pfeifer, B., U. Wittelsbürger, S. E. Ramos-Onsins, and M. J. Lercher. 2014. PopGenome: An
542 efficient swiss army knife for population genomic analyses in R. Mol Biol Evol. 31: 1929–36.
543
544 Phelan, J., F. Coll, R. McNerney, D. B. Ascher, D. E. V. Pires, *et al*. 2016. *Mycobacterium*
545 *tuberculosis* whole genome sequencing and protein structure modelling provides insights into
546 anti-tuberculosis drug resistance. BMC Med. 14: 31.
547
548 Renzette, N., S. P. Pfeifer, S. Matuszewski, T. F. Kowalik, and J. D. Jensen. 2017. On the
549 analysis of intrahost and interhost viral populations: human cytomegalovirus as a case study of
550 pitfalls and expectations. J Virol. 91: e01976-16.
551
552 Rocha, E. P. C., J. Maynard Smith, L.D. Hurst, M. T. G. Holden, J. E. Cooper, *et al*. 2006.
553 Comparisons of dN/dS are time dependent for closely related bacterial genomes. J Theor Biol.
554 239:226–35.
555
556 Sackman, A. M., R. B. Harris, and J.D. Jensen. 2019. Inferring demography and selection in
557 organisms characterized by skewed offspring distributions. Genetics. 211: 1019-1028.
558
559 Sherman, D. R., and S. Gagneux. 2011. Estimating the mutation rate of *Mycobacterium*
560 *tuberculosis* during infection. Nat Genet. 43: 400–401.
561
562 Tajima, F. 1989. Statistical method for testing the neutral mutation hypothesis by DNA
563 polymorphism. Genetics. 123: 585–595.
564
565 Tellier, A., and C. Lemaire. 2014. Coalescence 2.0: A multiple branching of recent theoretical
566 developments and their applications. Mol Ecol. 23: 2637–2652.
567
568 Thornton, K. R., J. D. Jensen, C. Becquet, and P. Andolfatto. 2007. Progress and prospects in
569 mapping recent selection in the genome. Heredity. 98: 340–348.
570
571 Trauner, A., Q. Liu, L. E. Via, X. Liu, X. Ruan, *et al*. 2017. The within-host population
572 dynamics of *Mycobacterium tuberculosis* vary with treatment efficacy. Genome Biol. 18: 71.

573 Vahey, M. D., and D. A. Fletcher. 2019. Low Fidelity Assembly of Influenza A Virus Promotes
574 Escape from Host Cells. Cell. 176: 281-294.

575 World Health Organization (WHO). 2018. Global tuberculosis report 2018. World Health
576 Organization, Geneva.
577

578

579

580

bioRxiv preprint doi: https://doi.org/10.1101/863894; this version posted December 4, 2019. The copyright holder for this preprint (which was not certified by peer review) is the author/funder. All rights reserved. No reuse allowed without permission.

Supporting Information

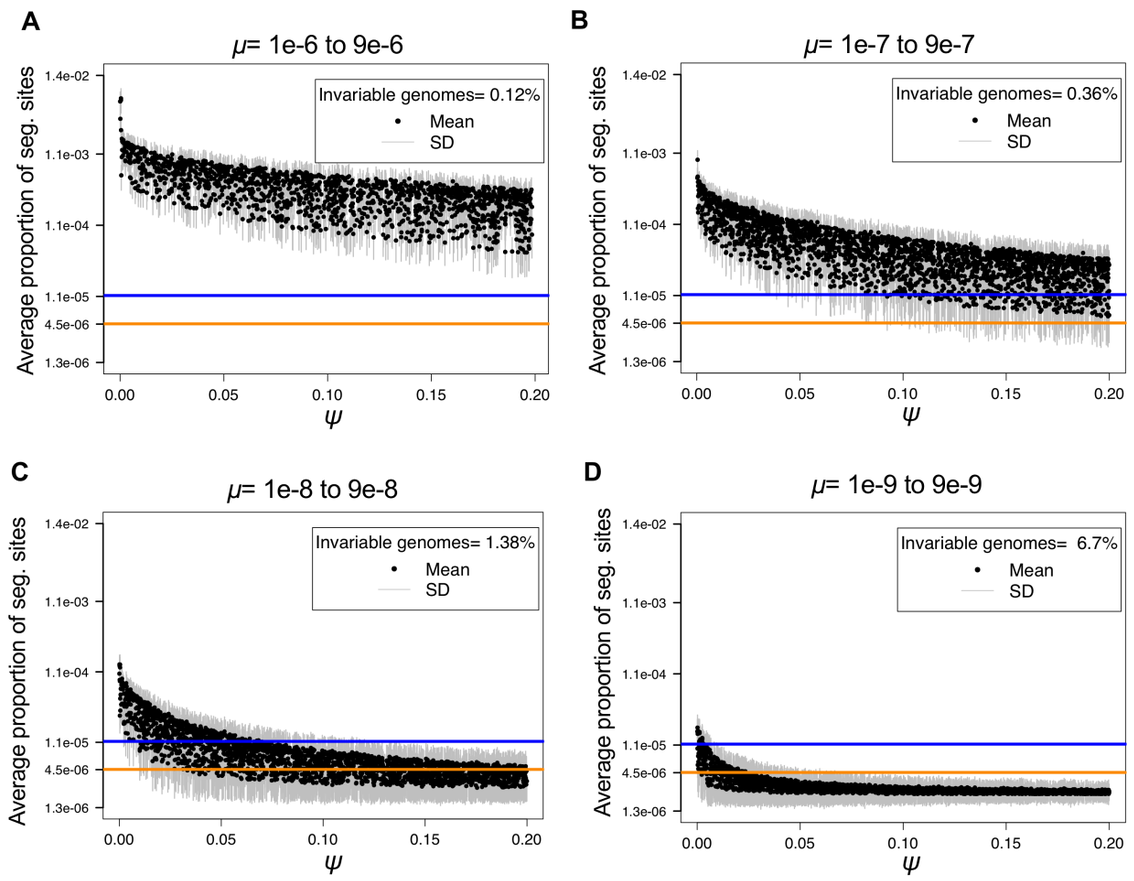


Figure S1. Log scale distribution of segregating sites in unfiltered simulated populations as a function of mutation rate (μ) and progeny skew (Ψ). For each parameter combination of μ and Ψ drawn from the prior (10,000 in total), 1,000 replicates were simulated, with the mean given by the black dot and the standard deviation given by the gray bars. Ψ proportions are given on the X-axis, while the proportion of segregating sites observed in the genome are given on the Y-axis. Each panel corresponds to a different order of magnitude of mutation rate: (A) 1e-6 to 9e-6, (B) 1e-7 to 9e-7, (C) 1e-8 to 9e-8, and (D) 1e-9 to 9e-9. The colored lines correspond to two examples of the proportion of segregating sites observed genome-wide in empirical patient data: 20 segregating sites as a mean (orange) and 50 segregating sites as the maximum observed from patient_10 (blue) (Trauner *et al.* 2017).

bioRxiv preprint doi: https://doi.org/10.1101/863894; this version posted December 4, 2019. The copyright holder for this preprint (which was not certified by peer review) is the author/funder. All rights reserved. No reuse allowed without permission.

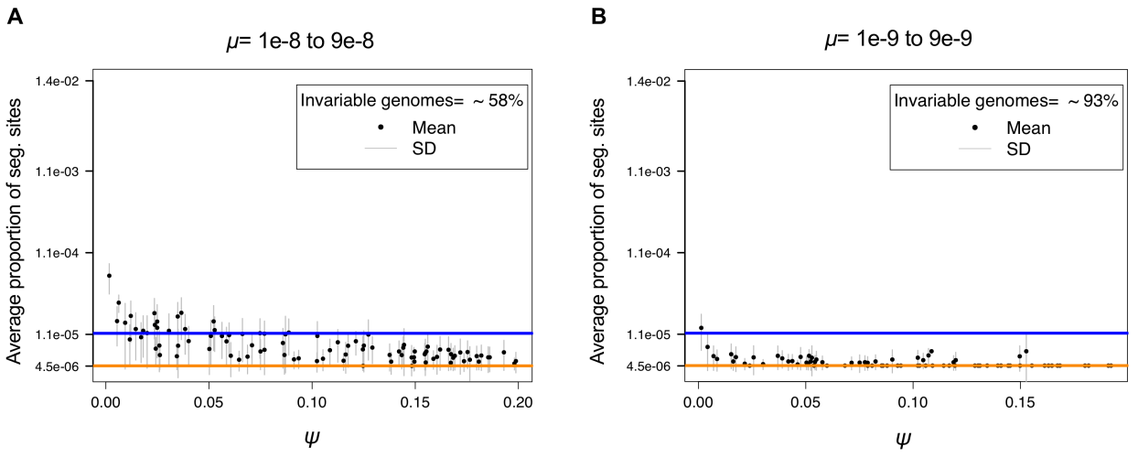
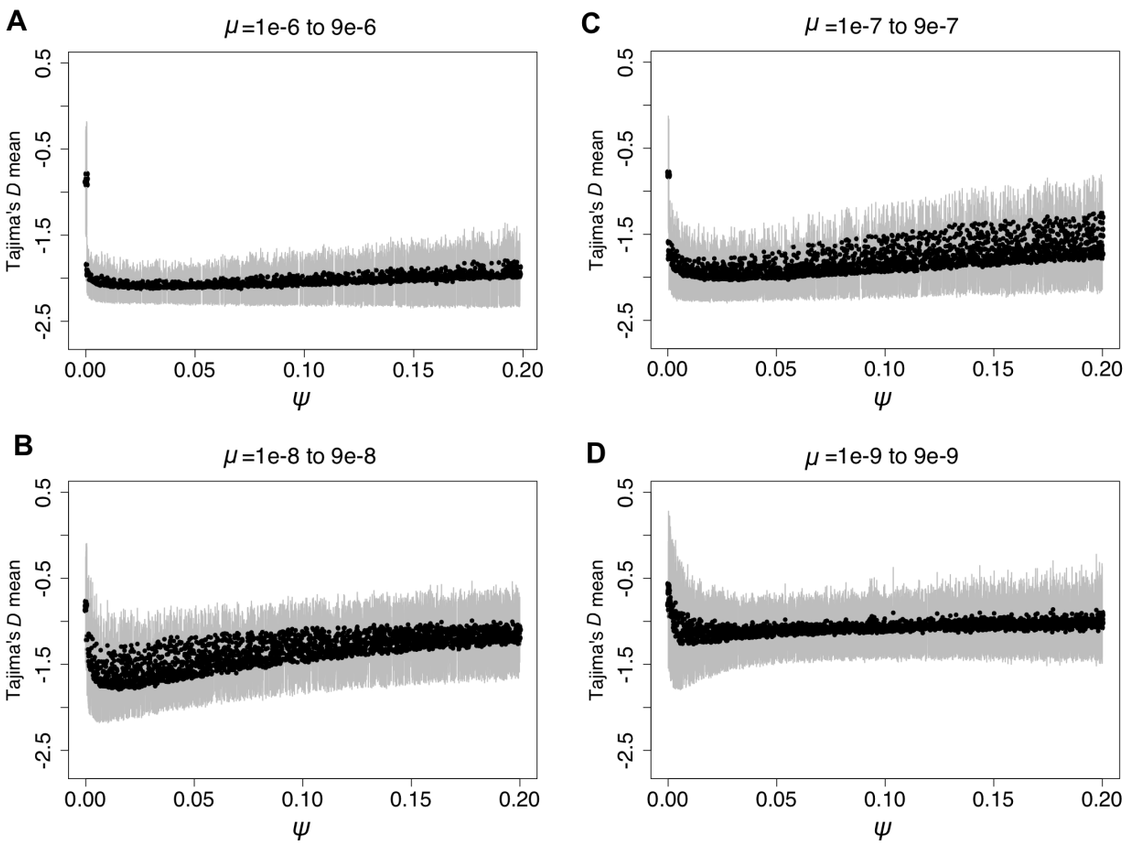


Figure S2. Log scale distribution of segregating sites in filtered simulated populations of *N* = 25,000 as a function of mutation rate (μ) and progeny skew (Ψ). For each parameter combination of μ and Ψ drawn from the prior (100 in total), 100 replicates were simulated, with the mean given by the black dot and the standard deviation given by the gray bars. Ψ proportions are given on the X-axis, while the proportion of segregating sites observed in the genome are given on the Y-axis. Each panel corresponds to a different order of magnitude of mutation rate: (A) 1e-8 to 9e-8, and (B) 1e-9 to 9e-9. The colored lines correspond to two examples of the proportion of segregating sites observed genome-wide in empirical patient data: 20 segregating sites (orange) and 50 segregating sites (blue) (Trauner *et al.* 2017). As shown, inference remains consistent with the results of Figure 2, even under this 25x larger population size.

bioRxiv preprint doi: https://doi.org/10.1101/863894; this version posted December 4, 2019. The copyright holder for this preprint (which was not certified by peer review) is the author/funder. All rights reserved. No reuse allowed without permission.



607

608 **Figure S3. The shape of the site frequency spectrum in unfiltered simulated populations, as**
609 **summarized by Tajima's *D*, as a function of mutation rate (μ) and progeny skew (Ψ).** For
610 each parameter combination of μ and Ψ drawn from the prior distributions (10,000 in total),
611 1,000 replicates were simulated, with the mean given by the black dot and the standard deviation
612 given by the gray bars. Ψ proportions are given on the X-axis, while the mean Tajima's *D* is
613 given on the Y-axis. Each panel corresponds to a different order of magnitude of mutation rate:
614 (A) 1e-6 to 9e-6, (B) 1e-7 to 9e-7, (C) 1e-8 to 9e-8, and (D) 1e-9 to 9e-9. As shown, the
615 distribution of variation expected to be observed in the genome differs as a function of these two
616 parameters - with a strong excess of rare mutations (negative *D*) observed as the WF model is
617 initially violated at small values of Ψ, with a slight recovery towards 0 (and larger standard
618 deviations) observed as Ψ gets larger, owing to the rapidly decreasing number of segregating
619 sites associated with increased progeny skew.

bioRxiv preprint doi: https://doi.org/10.1101/863894; this version posted December 4, 2019. The copyright holder for this preprint (which was not certified by peer review) is the author/funder. All rights reserved. No reuse allowed without permission.

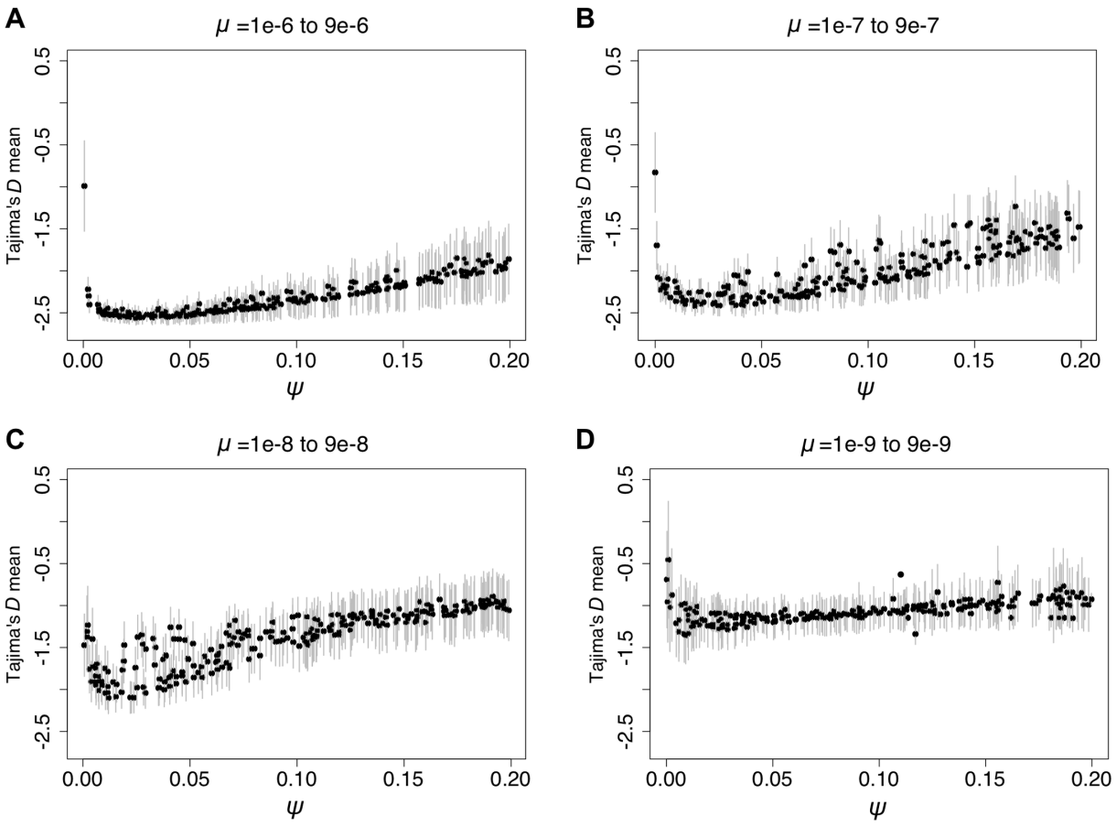


Figure S4. The shape of the site frequency spectrum (SFS), as summarized by Tajima's *D*, in simulated populations after filtering out segregating sites under 2% frequency, as a function of mutation rate (μ) and progeny skew (Ψ). 1,000 parameters combinations were used. For each parameter combination of μ and Ψ drawn from the prior distributions, 1,000 replicates were simulated, with the mean given by the black dot and the standard deviation given by the gray bars. Ψ proportions are given on the X-axis, while the mean Tajima's *D* is given on the Y-axis. Each panel corresponds to a different order of magnitude of mutation rate: (A) 1e-6 to 9e-6, (B) 1e-7 to 9e-7, (C) 1e-8 to 9e-8, and (D) 1e-9 to 9e-9. As shown, the distribution of variation expected to be observed in the genome differs as a function of these two parameters - with a strong excess of rare mutations (negative *D*) observed as the WF model is initially violated at small values of Ψ, with a slight recovery towards 0 (and larger standard deviations) observed as Ψ gets larger, owing to the rapidly decreasing number of segregating sites associated with increased progeny skew.

bioRxiv preprint doi: https://doi.org/10.1101/863894; this version posted December 4, 2019. The copyright holder for this preprint (which was not certified by peer review) is the author/funder. All rights reserved. No reuse allowed without permission.

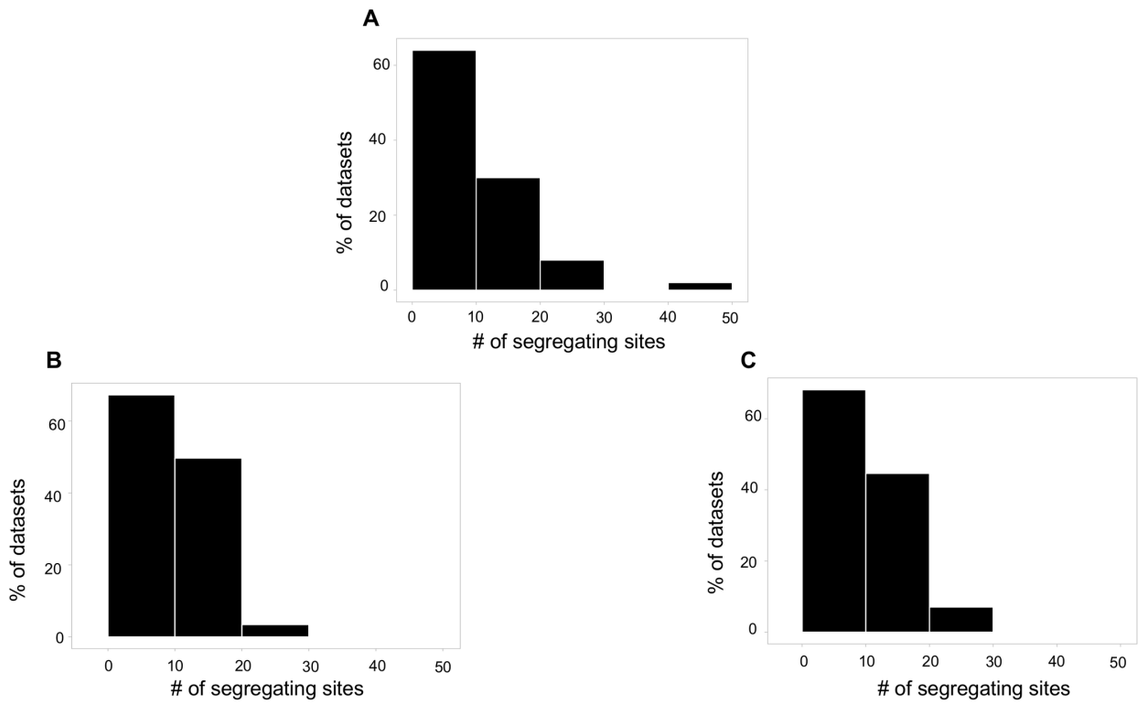


Figure S5. The distribution of segregating sites in real versus simulated datasets. Comparison of the number of segregating sites observed from (A) patient samples (Trauner *et al.* 2017) , (B) simulated datasets with μ = 3.1e-8 and Ψ = 0.02, resulting in the same mean number of segregating sites as observed in patients, and (C) simulated datasets with μ = 3.7e-7 and Ψ = 0.18, also resulting in the same mean number of segregating sites as observed in patients. Thus, these two point estimates essentially demarcate the boundaries on the joint posterior ridge (Figure 3).

bioRxiv preprint doi: https://doi.org/10.1101/863894; this version posted December 4, 2019. The copyright holder for this preprint (which was not certified by peer review) is the author/funder. All rights reserved. No reuse allowed without permission.

Table S1. Simulation results. Parameters simulated, ordered by descending mutation rate (μ) and corresponding values of progeny skew (Ψ) and bottleneck severity ($N2$). Given are the mean and standard deviation of the summary statistics from 1000 replicates.

Parameters			Summary statistics				
Mutation rate (μ)	**Progeny skew (ψ)**	**Bottle-neck ($N2$)**	**Tajima's *D* mean**	**Tajima's *D* sd**	**Seg. sites mean**	**Seg. Sites sd**	**% invariable genomes**
1.00323E-06	0.083741128	30	-2.268823115	0.213071226	73.25	27.92044146	0
1.05258E-06	0.05424026	51	-2.39378792	0.140975196	114.033	38.29559326	0
1.07427E-06	0.068391187	79	-2.342687183	0.150033316	62.118	22.00859956	0
1.14948E-06	0.174968669	27	-1.84867593	0.350954908	34.148	14.59140175	0
1.15893E-06	0.078976259	55	-2.314091665	0.187904351	87.857	32.7311454	0
1.16072E-06	0.147004609	47	-1.994103492	0.324323366	43.572	18.32666589	0
1.17846E-06	0.095707498	50	-2.242540595	0.219702856	74.732	27.21637204	0
1.21809E-06	0.002234156	94	-2.219989055	0.142920773	530.177	111.4160545	0
1.27435E-06	0.035230792	98	-2.45132687	0.111998152	184.69	55.9886652	0
1.34490E-06	0.072224963	2	-2.361174432	0.168335271	108.132	36.59953691	0
1.36631E-06	0.190031564	88	-1.814642081	0.40537193	36.049	15.11837174	0
1.37186E-06	0.178587611	8	-1.856448312	0.377166171	38.995	16.4323156	0
1.40763E-06	0.018259159	36	-2.459363944	0.105067026	299.336	81.75943805	0
1.41886E-06	0.048682507	78	-2.43334348	0.133550871	159.515	54.08471995	0
1.45413E-06	0.125929607	76	-2.130629042	0.278288809	65.433	24.43773135	0
1.49860E-06	0.034752818	87	-2.470499994	0.107467985	206.161	63.08506007	0
1.51763E-06	0.142547134	57	-2.068036111	0.303344227	58.533	21.69316723	0
1.51902E-06	0.127470119	5	-2.137500358	0.268938506	67.735	25.93629631	0
1.54224E-06	0.097141999	10	-2.252101995	0.212272889	91.618	33.4446501	0
1.56157E-06	0.127268671	73	-2.134927218	0.275793862	69.918	27.12203681	0
1.60310E-06	0.002535884	89	-2.300181435	0.120396219	581.913	125.9045805	0
1.60552E-06	0.114838011	13	-2.183291358	0.245635241	77.144	29.58409171	0
1.62498E-06	0.185445543	44	-1.873943114	0.390190692	43.922	18.62054351	0
1.70401E-06	0.079764023	56	-2.341980367	0.184901919	120.627	42.28086497	0
1.76944E-06	0.179382064	27	-1.909361982	0.369374432	48.587	21.04122535	0
1.79775E-06	0.006932201	87	-2.40224289	0.110270435	504.71	117.2538458	0
1.80560E-06	0.066056427	45	-2.399866678	0.146367114	150.828	51.46002867	0
1.81127E-06	0.172076915	37	-1.933554838	0.370411584	53.249	20.5200895	0
1.81152E-06	0.089215444	31	-2.320938106	0.183317642	115.119	41.23101789	0
1.81640E-06	0.011295921	70	-2.44570659	0.100980653	436.728	103.7460807	0
1.82390E-06	0.171978735	48	-1.941706405	0.363939575	54.583	21.79017951	0
1.86518E-06	0.103034261	72	-2.26005553	0.231646438	99.9	36.87109271	0
1.89217E-06	0.066288267	30	-2.406201331	0.157309604	156.594	51.49237447	0
1.90714E-06	0.07621348	53	-2.365034087	0.180909287	140.437	50.61689541	0
1.91685E-06	0.091231741	14	-2.319495906	0.20669643	119.203	41.9865295	0
1.98106E-06	0.071256528	25	-2.389881138	0.162727021	153.298	52.88578355	0
2.04999E-06	0.06206469	89	-2.427399389	0.142401025	173.69	56.74013873	0
2.09647E-06	0.038639738	42	-2.485880639	0.10741806	247.237	74.11912355	0
2.11204E-06	0.169388078	57	-1.984453843	0.330080624	48.27233429	17.97727958	30.6
2.12986E-06	0.11706933	77	-2.215467125	0.253808997	100.631	37.99700793	0
2.15406E-06	0.141870623	51	-2.10605375	0.274222571	58.14	22.20408569	0
2.18101E-06	0.163422243	18	-2.017817637	0.336968578	69.003	27.61317581	0
2.20091E-06	0.015172907	8	-2.477645048	0.094911447	427.758	106.3263595	0

bioRxiv preprint doi: https://doi.org/10.1101/863894; this version posted December 4, 2019. The copyright holder for this preprint (which was not certified by peer review) is the author/funder. All rights reserved. No reuse allowed without permission.

2.20482E-06	0.021126721	82	-2.491883563	0.09687563	365.716	102.0283643	0
2.20725E-06	0.188675008	28	-1.902430476	0.40017778	57.49	23.34714092	0
2.21559E-06	0.0871031	42	-2.343760706	0.186671872	139.264	49.71911397	0
2.23573E-06	0.187063106	45	-1.907741686	0.358805823	44.854	17.1103316	0
2.27509E-06	0.125403484	5	-2.203743064	0.23813124	98.003	36.40753355	0
2.27948E-06	0.137483753	32	-2.145546977	0.283584244	87.13	33.44340834	0
2.35400E-06	0.046762946	44	-2.475339189	0.123211173	236.372	73.3149828	0
2.52429E-06	0.191032835	83	-1.885597745	0.407044539	63.423	26.09231457	0
2.61389E-06	0.024278147	67	-2.503128139	0.091279236	385.128	108.5069277	0
2.66469E-06	0.143581712	59	-2.113962185	0.314452043	96.28	36.99459691	0
2.70701E-06	0.19942529	66	-1.86045003	0.416596013	64.021	25.95500378	0
2.73336E-06	0.025876486	80	-2.511972061	0.089679995	376.284	107.5730603	0
2.86631E-06	0.029798342	3	-2.521767014	0.080400891	166.654	52.68561529	0
2.87173E-06	0.142357014	34	-2.125391995	0.297032848	104.745	38.77612104	0
2.93144E-06	0.053739131	47	-2.465139706	0.132375425	251.39	82.07500354	0
2.94178E-06	0.096296588	12	-2.342917275	0.184995675	157.707	54.81443033	0
3.00818E-06	0.080858986	52	-2.394854503	0.172760168	187.604	66.3320822	0
3.01815E-06	0.134974227	3	-2.177646077	0.277538657	114.739	40.90511101	0
3.02499E-06	0.036913487	31	-2.506608647	0.103410471	325.834	102.6217992	0
3.02691E-06	0.099126233	97	-2.323489639	0.207079361	160.461	57.37567819	0
3.04722E-06	0.177489278	20	-1.996511616	0.345804407	82.887	33.44183888	0
3.08878E-06	0.166632161	47	-2.035520178	0.316529906	64.37974684	25.7113447	52.6
3.10911E-06	0.074397827	68	-2.423287664	0.162287959	208.453	73.55282326	0
3.15283E-06	0.105716416	97	-2.30220408	0.21672073	150.87	55.34531782	0
3.16156E-06	0.060129296	50	-2.470586921	0.129254198	246.51	82.18757021	0
3.18711E-06	0.187231211	95	-1.932400843	0.397556019	80.04	32.79457095	0
3.19924E-06	0.160557925	67	-2.075862881	0.323439171	98.938	36.62460263	0
3.21256E-06	0.197806677	97	-1.901179917	0.411388562	73.482	30.09819891	0
3.23557E-06	0.096667975	82	-2.33429967	0.203058174	171.881	60.98852711	0
3.23876E-06	0.032477714	5	-2.513252273	0.099558469	371.414	113.9971313	0
3.23960E-06	0.106816905	45	-2.299007369	0.227105568	155.651	57.23310954	0
3.25363E-06	0.010197306	81	-2.470389732	0.091743258	615.458	144.4888621	0
3.34148E-06	0.09036916	69	-2.360354627	0.183471731	188.152	66.35187614	0
3.38046E-06	0.075316468	10	-2.423214672	0.158800999	223.286	76.95137242	0
3.38234E-06	0.183560797	17	-1.992111459	0.318425592	62.81481481	24.34369074	56.8
3.43922E-06	0.052317077	29	-2.496508588	0.110215045	143.2914573	48.37521773	60.2
3.51100E-06	0.091190111	30	-2.36341697	0.189148653	191.025	66.20401307	0
3.62777E-06	0.174054427	62	-2.020730272	0.375769104	98.791	38.18973389	0
3.63591E-06	0.020922852	17	-2.523624462	0.086263393	491.719	134.7929344	0
3.71752E-06	0.007424968	35	-2.455211889	0.089901547	751.515	171.6138721	0
3.72700E-06	0.071519747	16	-2.439368425	0.144560149	246.579	84.58926115	0
3.76115E-06	0.133389599	45	-2.207183842	0.258449929	139.558	51.31061699	0
3.76891E-06	0.023000307	52	-2.525610163	0.084925102	479.201	133.0190688	0
3.77969E-06	0.058721949	18	-2.477337191	0.127971332	283.144	92.52348815	0
3.80658E-06	0.061662345	31	-2.456041954	0.134864962	271.953	91.58006169	0
3.81465E-06	0.043844958	47	-2.504175042	0.106799816	345.876	108.220702	0
3.85422E-06	0.045874048	89	-2.509525385	0.095470736	162.163	51.36789943	0
3.89087E-06	0.157624492	50	-2.100215392	0.317948113	117.258	45.17885085	0
3.92237E-06	0.105328979	66	-2.325915846	0.216457163	183.751	65.4317225	0
3.93140E-06	0.097279879	22	-2.348739672	0.199189136	197.806	70.31557896	0
4.05703E-06	0.081612311	27	-2.401847125	0.167117424	231.15	77.99177018	0
4.06679E-06	0.052914714	99	-2.49677306	0.114718297	320.979	100.8842713	0

bioRxiv preprint doi: https://doi.org/10.1101/863894; this version posted December 4, 2019. The copyright holder for this preprint (which was not certified by peer review) is the author/funder. All rights reserved. No reuse allowed without permission.

4.08698E-06	0.162083695	39	-2.082530637	0.338399342	119.814	46.42963617	0
4.11463E-06	0.147405055	97	-2.161054228	0.286645225	136.814	51.00116197	0
4.13130E-06	0.071193318	91	-2.450204823	0.139381082	261.729	88.2090494	0
4.13286E-06	0.178097374	72	-2.005132374	0.379378644	104.374	41.08281784	0
4.13787E-06	0.183625187	25	-1.98190994	0.385122469	105.096	42.00653917	0
4.18713E-06	0.115383656	91	-2.279541427	0.233838275	177.233	61.31608576	0
4.21578E-06	0.063481085	74	-2.465993109	0.131570546	283.843	93.59634944	0
4.22855E-06	0.044531836	24	-2.514562421	0.10546776	365.052	116.1490934	0
4.26758E-06	0.064487967	61	-2.466350062	0.137762942	292.162	96.33562326	0
4.27081E-06	0.057983672	56	-2.480132515	0.126682888	310.77	98.58679656	0
4.27458E-06	0.051484956	70	-2.502621768	0.119753276	341.951	109.9885725	0
4.28112E-06	0.081497163	85	-2.414976591	0.172164667	245.994	82.79997464	0
4.33473E-06	0.18325412	16	-1.996033612	0.346812486	73.077	28.78485085	0
4.34382E-06	0.089599967	85	-2.389938479	0.160930254	126.775	44.33068446	0
4.35363E-06	0.031937187	16	-2.533881587	0.088578631	441.809	130.8727863	0
4.38638E-06	0.170332639	1	-2.043150239	0.357100011	121.465	47.98244565	0
4.40373E-06	0.180950653	97	-2.02066542	0.34257131	112.818	44.79637922	0
4.44451E-06	0.009495684	39	-2.48671751	0.089372565	763.837	181.69039	0
4.46435E-06	0.06388055	45	-2.476451069	0.114443462	152.5642633	51.75499953	68.1
4.66398E-06	0.161534783	2	-2.101108883	0.320353546	88.532	32.16074143	0
4.67889E-06	0.147050753	36	-2.166447463	0.301217068	148.635	55.85450296	0
4.68696E-06	0.159150751	5	-2.118221146	0.316422699	135.536	51.71722513	0
4.69022E-06	0.179421998	68	-2.007102216	0.375179908	119.294	47.68985097	0
4.76545E-06	0.137827068	66	-2.198064664	0.283620018	163.71	60.01127605	0
4.82616E-06	0.09864471	54	-2.360936732	0.198095182	226.198	78.88992595	0
4.90490E-06	0.068348785	36	-2.463883915	0.137071673	309.916	98.59704012	0
4.92672E-06	0.037491836	45	-2.53464184	0.089585124	437.73	134.1963254	0
4.96090E-06	0.194931247	66	-1.943824358	0.406728845	111.012	45.51902721	0
4.99886E-06	0.084205461	81	-2.415349811	0.164869693	271.626	90.2507802	0
5.03965E-06	0.010818434	41	-2.502006876	0.084952354	765.118	187.5172814	0
5.08458E-06	0.092243176	67	-2.395655224	0.168627216	137.778	50.38058077	0
5.19177E-06	0.081319929	51	-2.423738507	0.158052048	279.023	94.15976068	0
5.19312E-06	0.177636988	13	-2.014820856	0.373052196	131.709	50.46064403	0
5.28653E-06	0.159011493	5	-2.111142553	0.312880421	151.001	57.19405703	0
5.33565E-06	0.036433081	70	-2.536428429	0.093074865	466.303	140.9724811	0
5.34859E-06	0.032126559	79	-2.536982301	0.092139694	502.513	146.1721866	0
5.34876E-06	0.074147757	73	-2.446396385	0.141400751	307.527	98.73268666	0
5.37165E-06	0.070847357	98	-2.464197299	0.14237841	318.068	106.417687	0
5.39080E-06	0.148057423	61	-2.17056632	0.291890977	164.095	58.76678918	0
5.42598E-06	0.033790744	76	-2.537953881	0.090863628	490.955	145.8321981	0
5.45932E-06	0.150455894	94	-2.138987203	0.303190167	163.692	61.6935753	0
5.49750E-06	0.013493694	73	-2.51213801	0.084049365	745.896	194.3784818	0
5.50896E-06	0.148013485	41	-2.179766751	0.27981175	171.601	64.51595235	0
5.52108E-06	0.017269882	8	-2.530306408	0.085229634	680.684	183.9934285	0
5.59879E-06	0.079697476	68	-2.42298135	0.161658037	302.269	106.0762877	0
5.61346E-06	0.039363853	66	-2.533772282	0.099950806	457.639	145.3699457	0
5.62852E-06	0.134515261	5	-2.229571912	0.254274997	187.168	68.44351167	0
5.63844E-06	0.165350342	49	-2.092404381	0.342592855	154.336	57.47631365	0
5.64346E-06	0.197158598	52	-1.948358035	0.406635491	120.541	47.30573064	0
5.66941E-06	0.014846757	37	-2.527392022	0.084809703	731.887	186.8805516	0
5.77125E-06	0.039009255	20	-2.534196812	0.096215357	475.949095	151.0681737	11.6
5.79828E-06	0.102032778	31	-2.347687999	0.215802247	252.055	87.4202853	0

bioRxiv preprint doi: https://doi.org/10.1101/863894; this version posted December 4, 2019. The copyright holder for this preprint (which was not certified by peer review) is the author/funder. All rights reserved. No reuse allowed without permission.

5.81859E-06	0.018901769	41	-2.536851337	0.081223929	670.963	187.6406316	0
5.86554E-06	0.119172716	42	-2.289135668	0.247164645	224.895	80.54838308	0
5.87513E-06	0.009945494	12	-2.529829888	0.065175172	354.518	90.49086292	0
5.91748E-06	0.108639825	8	-2.330618799	0.21801644	245.334	89.73793702	0
5.95191E-06	0.163364246	88	-2.0916936	0.343509769	159.667	63.38283281	0
5.96091E-06	0.087444079	18	-2.41819886	0.161575551	153.277	55.05082074	0
5.99521E-06	0.181327866	30	-2.035142738	0.356564966	144.429	55.8730414	0
6.01869E-06	0.177907004	55	-2.06257483	0.326697733	147.444	57.72470013	0
6.05063E-06	0.002877447	32	-2.401946034	0.096067514	1198.869	255.7148841	0
6.07731E-06	0.01955547	1	-2.541352169	0.080011363	681.491	179.4129955	0
6.14328E-06	0.060748557	55	-2.49084606	0.129369442	383.209	129.8532063	0
6.21723E-06	0.043054603	2	-2.532038626	0.097144385	474.703	147.9193257	0
6.22292E-06	0.051537806	68	-2.522713259	0.107135081	422.113	136.9644972	0
6.28351E-06	0.04833965	58	-2.528331181	0.102515432	449.096	145.2344237	0
6.28653E-06	0.081165105	44	-2.431136744	0.155267755	321.523	106.133132	0
6.32747E-06	0.193498773	51	-2.01025924	0.377904736	138.227	54.61023484	0
6.34468E-06	0.027728583	71	-2.553733432	0.080758412	581.877	172.5323601	0
6.34891E-06	0.09256866	32	-2.398773229	0.179032918	295.067	100.3194124	0
6.36937E-06	0.142826501	50	-2.200359147	0.272622369	120.961	46.28833643	0
6.39225E-06	0.000498444	97	-0.990254509	0.538172921	4711.724	1154.140446	0
6.42691E-06	0.049874555	75	-2.520309606	0.10979855	442.701	142.79228	0
6.42861E-06	0.063886961	7	-2.490548155	0.131109928	390.055	130.0545045	0
6.45845E-06	0.039415139	19	-2.541081406	0.094079965	511.883	159.5622745	0
6.50933E-06	0.061705597	79	-2.493064687	0.123437591	389.011	123.4561878	0
6.52081E-06	0.179715526	95	-2.052669741	0.347732189	158.22	61.28929742	0
6.61941E-06	0.013406386	49	-2.527695803	0.076238044	840.509	207.1711655	0
6.67778E-06	0.025203094	41	-2.552025842	0.083223018	643.11	184.4100349	0
6.71129E-06	0.184675108	81	-2.033468914	0.36471217	157.084	59.45143747	0
6.74110E-06	0.012953563	72	-2.529307254	0.078355505	870.143	224.0870893	0
6.77895E-06	0.042308741	80	-2.541125362	0.090781076	497.057	147.9309884	0
6.78473E-06	0.180034226	47	-2.037501557	0.354121272	163.303	62.91191541	0
6.80869E-06	0.146559555	21	-2.19406396	0.284609993	122.693	45.58109682	0
6.82733E-06	0.056909954	59	-2.513305204	0.113574939	422.41	134.0480988	0
6.83593E-06	0.076868611	49	-2.442675613	0.160653802	350.257	118.3542592	0
6.84453E-06	0.025937913	15	-2.556708238	0.078860856	644.687	193.0205065	0
6.86818E-06	0.088019082	47	-2.420797254	0.179780326	320.616	104.4551072	0
6.90801E-06	0.007457312	75	-2.48893408	0.080148005	1048.332	239.3597562	0
6.95230E-06	0.186057268	78	-2.018813781	0.350502131	157.646	60.18999518	0
6.98195E-06	0.150790823	8	-2.173780372	0.296051761	201.855	76.85593542	0
7.01129E-06	0.117400419	99	-2.317364359	0.223678581	260.326	92.96620052	0
7.02328E-06	0.062670765	68	-2.495649631	0.12599538	408.589	129.633317	0
7.03960E-06	0.076898129	49	-2.458608975	0.144983134	369.077	124.3281326	0
7.04110E-06	0.02039321	27	-2.551816517	0.073694819	739.155	201.868308	0
7.07798E-06	0.09952533	11	-2.367716285	0.202708985	298.488	106.8031028	0
7.16578E-06	0.164836135	34	-2.112573648	0.324466583	189.619	73.83079863	0
7.16907E-06	0.178343668	30	-2.06332979	0.329153933	112.1597938	39.12594559	80.6
7.17772E-06	0.138474662	21	-2.229724935	0.26582104	230.211	79.97094367	0
7.18952E-06	0.051417423	58	-2.529305237	0.107858519	474.913	150.5340624	0
7.21034E-06	0.131057148	41	-2.263690883	0.236809421	238.425	84.12810418	0
7.21766E-06	0.150426253	89	-2.183733977	0.30257552	210.568	80.25684106	0
7.22276E-06	0.065801281	27	-2.487010759	0.135017996	395.223	131.0033326	0
7.28827E-06	0.054523495	28	-2.512510853	0.117947502	447.441	148.2902712	0

bioRxiv preprint doi: https://doi.org/10.1101/863894; this version posted December 4, 2019. The copyright holder for this preprint (which was not certified by peer review) is the author/funder. All rights reserved. No reuse allowed without permission.

7.34886E-06	0.048310702	34	-2.530371191	0.106199965	494.59	158.0397053	0
7.36520E-06	0.051301492	95	-2.51914289	0.113994345	472.227	147.7385398	0
7.39311E-06	0.048410189	44	-2.543515174	0.089002604	222.213	75.67403908	0
7.39443E-06	0.142488828	65	-2.223760785	0.272916523	228.38	82.59871759	0
7.41247E-06	0.082466592	26	-2.445896823	0.155609023	350.58	127.4844614	0
7.42439E-06	0.138494135	4	-2.226955385	0.279720187	232.196	84.05707094	0
7.50443E-06	0.074608316	53	-2.467081169	0.144974333	380.4653266	126.8435385	0.5
7.51767E-06	0.137078511	72	-2.245032333	0.257150794	236.178	86.07827708	0
7.59875E-06	0.04001344	92	-2.548634304	0.094289806	549.201	174.9091301	0
7.60124E-06	0.197655797	56	-1.971468748	0.394631373	160.586	61.63470971	0
7.64061E-06	0.075298103	79	-2.459775663	0.156429417	386.462	132.3871252	0
7.68735E-06	0.086217638	71	-2.447923552	0.143747413	179.422	63.82486608	0
7.73333E-06	0.079299325	79	-2.452550733	0.15307327	376.58	127.8387983	0
7.77212E-06	0.196554711	63	-1.984723902	0.392655194	164.695	63.20779382	0
7.80427E-06	0.011199664	63	-2.520420468	0.077848821	966.524	235.7493355	0
7.86550E-06	0.179721627	71	-2.06962471	0.341131207	181.521	69.42190548	0
7.88451E-06	0.080996722	35	-2.449756283	0.153657455	383.829	133.0214662	0
7.88638E-06	0.1666448	59	-2.120404744	0.322095976	201.396	75.09448959	0
7.92294E-06	0.067269241	93	-2.485810753	0.13481249	418.795	138.7381103	0
7.98441E-06	0.061223256	13	-2.506154325	0.119019726	451.1435794	146.2317971	1.1
7.99095E-06	0.089447718	53	-2.440670425	0.149941216	179.837	65.68188899	0
7.99285E-06	0.050713501	97	-2.534753003	0.106458715	495.403	155.9264623	0
7.99901E-06	0.050967349	89	-2.528929069	0.103038136	497.634	154.4307252	0
8.00013E-06	0.128142071	83	-2.277511989	0.24697584	268.947	96.30920857	0
8.00249E-06	0.11790393	55	-2.322167818	0.227962689	288.982	97.69893939	0
8.00836E-06	0.148077971	87	-2.199919025	0.284032144	136.619	48.85972894	0
8.11586E-06	0.167457995	87	-2.132365478	0.320822963	124.238	46.64501166	0
8.13033E-06	0.021430876	75	-2.551283793	0.079865134	773.333	207.6434538	0
8.17407E-06	0.125348653	80	-2.284101759	0.239945517	276.9866518	96.61832147	10.1
8.27083E-06	0.074989706	45	-2.464181313	0.152911371	413.274	143.7678619	0
8.29799E-06	0.024720669	88	-2.566448744	0.079759978	719.667	211.7515214	0
8.30624E-06	0.104965581	65	-2.363483165	0.200270093	321.74	112.5569521	0
8.44438E-06	0.186754651	80	-2.018784115	0.383265374	188.768	72.4658366	0
8.46443E-06	0.101071854	5	-2.378379641	0.2010005	335.763	113.2412664	0
8.46703E-06	0.165195627	75	-2.129612837	0.31867126	216.681	83.37253876	0
8.46893E-06	0.032363037	37	-2.55913469	0.082819055	653.552	201.7541525	0
8.49289E-06	0.052155964	70	-2.529301194	0.10687454	511.329	168.0613977	0
8.49640E-06	0.011483327	93	-2.524171765	0.077585068	995.999	253.6725029	0
8.50168E-06	0.157491798	58	-2.150882271	0.3135751	224.714	82.46358255	0
8.59353E-06	0.119391729	2	-2.310786869	0.233170398	301.436	110.8122613	0
8.63529E-06	0.112601893	34	-2.331966464	0.228850405	313.448	111.5213805	0
8.64280E-06	0.128128245	19	-2.258019263	0.255049042	281.851	100.7786641	0
8.72579E-06	0.133745637	41	-2.247429925	0.277316686	270.206	100.7595854	0
8.73167E-06	0.021543106	22	-2.552923449	0.082063861	785.933	223.020202	0
8.74277E-06	0.017176358	80	-2.549018151	0.076780648	864.539	242.7295081	0
8.77671E-06	0.116429936	1	-2.323459329	0.237454452	310.695	109.1745715	0
8.79343E-06	0.103772443	78	-2.376890594	0.188639046	335.424	119.675923	0
8.80503E-06	0.009299307	97	-2.515949453	0.075308786	1085.272	272.3681046	0
8.81455E-06	0.039320445	79	-2.555134061	0.092649516	612.422	203.4150181	0
8.84282E-06	0.113147577	88	-2.342495118	0.20960697	319.741	108.2580053	0
8.89345E-06	0.045187261	8	-2.543956231	0.098464532	560.6888658	173.7109308	3.9
1.01007E-07	0.037207555	42	-2.051728712	0.197389059	21.65	8.301229452	0

bioRxiv preprint doi: https://doi.org/10.1101/863894; this version posted December 4, 2019. The copyright holder for this preprint (which was not certified by peer review) is the author/funder. All rights reserved. No reuse allowed without permission.

1.06501E-07	0.043483318	60	-2.012139803	0.212294591	19.3993994	7.609036372	0.1
1.11486E-07	0.038947139	4	-2.059089214	0.203824726	22.616	8.495217049	0
1.16237E-07	0.086858593	96	-1.690919447	0.28940054	9.419715447	4.341671266	1.6
1.30883E-07	0.082461751	26	-1.76546852	0.281696443	11.30251256	5.274167687	0.5
1.31513E-07	0.169136567	32	-1.235420133	0.365639957	4.790486976	2.412702611	11.7
1.31540E-07	0.073409472	70	-1.865148747	0.25371201	13.37951807	5.777146291	0.4
1.31617E-07	0.009450759	77	-2.125155336	0.185832109	76.434	19.25191628	0
1.34829E-07	0.000769518	77	-1.697173636	0.284645295	136.115	30.2327934	0
1.38570E-07	0.084078144	44	-1.780101152	0.272122944	11.87638191	5.493346531	0.5
1.43412E-07	0.105046852	85	-1.637557995	0.301087978	9.364646465	4.619753891	1
1.46392E-07	0.040145492	17	-2.135284109	0.184647437	28.418	10.39332946	0
1.48040E-07	0.005775423	78	-2.098596342	0.182797238	98.163	24.08057942	0
1.51325E-07	0.105622891	79	-1.670288298	0.312594453	9.773373984	4.550212945	1.6
1.53729E-07	0.034102996	71	-2.178654623	0.172540664	34.491	11.81259736	0
1.55198E-07	0.032455678	97	-2.191126512	0.173775225	37.506	12.53375678	0
1.56929E-07	0.057293669	13	-2.042616833	0.20408599	20.968	8.100283365	0
1.58551E-07	0.090848716	65	-1.769475169	0.281742653	12.20523139	5.734485422	0.6
1.59398E-07	0.140382942	9	-1.456672525	0.367980397	7.033057851	3.521384245	3.2
1.61103E-07	0.070249371	69	-1.936668307	0.248297836	17.00801603	7.294076125	0.2
1.61814E-07	0.147711891	83	-1.431511401	0.330481489	6.719334719	3.289408534	3.8
1.64562E-07	0.034303216	59	-2.204674548	0.164424981	37.408	12.50815694	0
1.64607E-07	0.04166588	29	-2.148898671	0.186285207	30.243	10.84147077	0
1.67115E-07	0.042028676	83	-2.158735481	0.171895398	30.332	11.00776757	0
1.72210E-07	0.160113083	69	-1.396790625	0.351619853	6.412147505	3.224058574	7.8
1.75415E-07	0.104000951	12	-1.740389559	0.287249414	11.67507568	5.48417138	0.9
1.81932E-07	0.14681816	88	-1.461909975	0.35936019	7.61761658	3.760172995	3.5
1.83192E-07	0.021043343	23	-2.251400713	0.149714884	60.754	17.8018648	0
1.88713E-07	0.156515898	48	-1.392182677	0.381506499	7.013569937	3.69342713	4.2
1.90009E-07	0.021541516	89	-2.248712907	0.155683169	59.158	17.47599629	0
1.91987E-07	0.010356717	30	-2.202204033	0.168264635	97.794	24.93181019	0
1.93567E-07	0.020632953	51	-2.252492364	0.155272094	63.037	18.30378812	0
2.03309E-07	0.157051872	34	-1.456888632	0.381325772	7.923879041	4.091776361	4.1
2.18721E-07	0.086025658	74	-1.924202682	0.263315314	17.60760761	7.361151764	0.1
2.19485E-07	0.032888251	27	-2.256192839	0.153005715	49.268	15.75983974	0
2.19679E-07	0.154142694	77	-1.495808435	0.371576186	8.616803279	4.153797697	2.4
2.22485E-07	0.126848726	43	-1.647251953	0.32377229	10.78947368	5.211262308	1.2
2.25032E-07	0.155844325	48	-1.480786984	0.373873978	8.399795501	4.352986946	2.2
2.29831E-07	0.030077451	71	-2.27335215	0.143059314	55.338	18.12904902	0
2.31006E-07	0.016107215	84	-2.263564921	0.153668533	84.815	22.90955309	0
2.42615E-07	0.094599317	40	-1.899536017	0.269312799	17.18336673	7.410681378	0.2
2.44791E-07	0.024944146	43	-2.286677176	0.146057109	68.256	21.01609241	0
2.45494E-07	0.029922845	11	-2.284437618	0.152107372	58.574	18.39992068	0
2.48791E-07	0.157492765	73	-1.527458089	0.351890945	9.229441624	4.561475544	1.5
2.52080E-07	0.193546788	21	-1.31359069	0.38831406	7.111461619	3.590365041	4.9
2.54351E-07	0.032071962	69	-2.281012588	0.151163693	56.094	18.23056547	0
2.55051E-07	0.115715145	62	-1.808019754	0.283378053	14.54929577	6.527043788	0.6
2.56097E-07	0.068202216	46	-2.099016583	0.221928491	27.858	11.27656849	0
2.57110E-07	0.130054995	61	-1.693241351	0.337814069	12.3919598	5.889930677	0.5
2.60855E-07	0.134972889	90	-1.676219507	0.334868692	11.80524723	5.582205921	0.9
2.65494E-07	0.159940203	68	-1.522496241	0.359625464	9.347560976	4.465207894	1.6
2.66887E-07	0.137423897	27	-1.656033391	0.335390019	11.62273642	5.640231523	0.6
2.67293E-07	0.178332191	26	-1.429277855	0.390284363	8.269270298	4.152624633	2.7

bioRxiv preprint doi: https://doi.org/10.1101/863894; this version posted December 4, 2019. The copyright holder for this preprint (which was not certified by peer review) is the author/funder. All rights reserved. No reuse allowed without permission.

2.67657E-07	0.01171703	22	-2.26184749	0.151632922	115.415	29.1269833	0
2.77101E-07	0.089815698	84	-1.97863907	0.262622641	21.281	8.637629747	0
2.84542E-07	0.159657855	67	-1.551669886	0.360559259	10.24696356	4.913614534	1.2
2.86705E-07	0.076434857	35	-2.080676078	0.217220878	27.147	10.96565715	0
2.95952E-07	0.009966019	61	-2.262246359	0.151047832	135.232	32.51974338	0
2.98885E-07	0.121334637	44	-1.800200899	0.322363033	15.65295888	6.952934414	0.3
3.00067E-07	0.194122681	2	-1.381106528	0.400836709	8.141675284	4.106449818	3.3
3.02974E-07	0.089504202	68	-2.002698716	0.24189679	23.6	9.763879011	0
3.20559E-07	0.088571362	72	-2.015069109	0.256241002	24.705	10.17799423	0
3.22863E-07	0.097689633	25	-1.993466538	0.243670378	22.576	9.420348559	0
3.26118E-07	0.036476882	14	-2.303960911	0.146584594	62.736	21.17547413	0
3.27505E-07	0.005282555	41	-2.179380302	0.166583287	186.832	40.77330301	0
3.29323E-07	0.050551651	60	-2.253900919	0.177992937	46.379	16.37392636	0
3.29820E-07	0.067238279	28	-2.163622197	0.191617613	34.587	12.93598743	0
3.30007E-07	0.156793492	89	-1.617907817	0.357900941	11.94869215	5.81767139	0.6
3.35742E-07	0.167702541	54	-1.548066791	0.381756124	10.81010101	5.146027259	1
3.41295E-07	0.173539696	52	-1.533585629	0.380551779	10.71890799	5.294739619	1.1
3.42671E-07	0.082308406	83	-2.089385281	0.218527615	28.736	11.30673013	0
3.42882E-07	0.07431508	8	-2.121981096	0.225706387	32.72	12.81154697	0
3.45360E-07	0.042748883	49	-2.288643438	0.158097015	56.221	19.0995013	0
3.58661E-07	0.07559624	28	-2.134153711	0.208705032	33.103	13.04954718	0
3.59921E-07	0.125055574	99	-1.829067947	0.310160581	17.93881645	7.852765852	0.3
3.61200E-07	0.166728483	96	-1.59625845	0.370273383	12.28830645	5.890828558	0.8
3.61990E-07	0.115642209	19	-1.894221514	0.304138975	19.73073073	8.826686091	0.1
3.67849E-07	0.088095933	67	-2.072838478	0.234517588	28.558	10.95968753	0
3.71272E-07	0.180958839	47	-1.509631867	0.405640517	11.18705763	5.698781241	1.1
3.71916E-07	0.185370158	53	-1.470742075	0.395973823	10.56275304	5.375005885	1.2
3.75708E-07	0.059146015	60	-2.242430884	0.17534194	45.729	16.15718458	0
3.79205E-07	0.126706296	27	-1.841558912	0.298893032	18.514	7.936043396	0
3.81526E-07	0.012531531	55	-2.309963075	0.145753473	143.198	36.64332858	0
3.81531E-07	0.184663853	87	-1.482191711	0.425535539	10.89292929	5.422181394	1
3.84650E-07	0.035590645	80	-2.327969953	0.151926452	72.516	22.81864226	0
3.85416E-07	0.175953718	53	-1.563247984	0.378332212	11.71039354	5.718645999	0.9
3.86830E-07	0.106141973	46	-1.974307014	0.262384794	23.65	9.968092238	0
3.88749E-07	0.079953214	58	-2.147676944	0.205784745	33.827	13.18950469	0
3.88788E-07	0.04436575	64	-2.310322328	0.154710767	61.693	20.85727156	0
3.90501E-07	0.058404112	96	-2.240043769	0.172156923	47.056	17.70271872	0
3.91166E-07	0.138171295	90	-1.790899531	0.327033394	17.18336673	7.311759663	0.2
3.92821E-07	0.003985377	82	-2.168462609	0.162018642	224.207	47.82461024	0
3.93391E-07	0.041200387	66	-2.312058383	0.156169676	66.356	21.61935847	0
4.02929E-07	0.169936849	3	-1.603446846	0.381425273	13.05236657	6.586679873	0.7
4.11887E-07	0.06560143	87	-2.215498124	0.188134209	43.547	16.05270944	0
4.14708E-07	0.110029495	25	-1.959219285	0.266771854	23.897	10.10467691	0
4.18398E-07	0.171023922	9	-1.628216432	0.35684027	13.5427996	6.409924184	0.7
4.20551E-07	0.090051366	33	-2.096146008	0.224228824	31.441	12.4585607	0
4.25340E-07	0.137870962	64	-1.812475466	0.31592473	18.34068136	8.114536675	0.2
4.26358E-07	0.166239545	10	-1.662961204	0.374864082	14.6252505	6.943376348	0.2
4.28101E-07	0.158786361	54	-1.70345215	0.351579083	15.60621242	7.121825798	0.2
4.30122E-07	0.141437011	3	-1.781114828	0.325992818	17.60140562	7.776058995	0.4
4.34453E-07	0.18849351	70	-1.524455338	0.407446459	11.95766129	5.741155772	0.8
4.42454E-07	0.017329756	89	-2.347727504	0.132725352	136.154	36.57126935	0
4.44893E-07	0.169470657	8	-1.641322354	0.354117793	14.17570281	6.560752194	0.4

bioRxiv preprint doi: https://doi.org/10.1101/863894; this version posted December 4, 2019. The copyright holder for this preprint (which was not certified by peer review) is the author/funder. All rights reserved. No reuse allowed without permission.

4.48038E-07	0.004796206	91	-2.212677756	0.159731975	231.579	51.24767393	0
4.52654E-07	0.186283576	46	-1.552785915	0.393812293	12.62825651	6.178479099	0.2
4.56315E-07	0.181095092	36	-1.590898111	0.399559542	13.17771084	6.001804183	0.4
4.56356E-07	0.199225753	72	-1.476786266	0.423571001	11.66565962	5.78452111	0.7
4.57230E-07	0.151610343	43	-1.732066618	0.384118326	17.00900901	7.852403415	0.1
4.57358E-07	0.187871408	27	-1.534098368	0.422468046	12.70251256	6.327413428	0.5
4.58596E-07	0.116048413	48	-1.961712174	0.280322732	25.57057057	10.3504124	0.1
4.59638E-07	0.053993528	73	-2.300837062	0.154081865	59.535	20.63842823	0
4.65103E-07	0.116094108	28	-1.962340759	0.291183615	25.40280561	10.54103469	0.2
4.66800E-07	0.161534222	85	-1.695431883	0.380400702	16.03106212	7.387133836	0.2
4.72373E-07	0.105331015	61	-2.04391141	0.258162119	29.021	11.77017825	0
4.73611E-07	0.013217151	99	-2.338045263	0.130808871	167.561	42.67612366	0
4.74453E-07	0.075842681	41	-2.201958167	0.183824769	41.642	15.26974135	0
4.76678E-07	1.81E-05	80	-0.828796119	0.473864262	627.398	139.04378	0
4.78537E-07	0.179169857	19	-1.606507287	0.406218549	14.59337349	6.715489952	0.4
4.81157E-07	0.160491168	58	-1.72225111	0.350772212	16.67667668	7.844465427	0.1
4.85082E-07	0.137902666	4	-1.857548224	0.324507283	20.85785786	9.237992033	0.1
4.85231E-07	0.183335963	55	-1.609872234	0.373760088	14.39034205	6.840032868	0.6
4.86011E-07	0.131413846	12	-1.881475385	0.307215953	22.098	9.195812034	0
4.86422E-07	0.022695217	3	-2.373722617	0.125346109	123.777	35.01578753	0
4.87254E-07	0.01990165	26	-2.36873971	0.123626619	134.026	38.07943497	0
4.89744E-07	0.098521639	81	-2.077731826	0.223896387	31.116	12.53098438	0
4.92587E-07	0.198861697	51	-1.479313208	0.433173479	12.18932528	5.880737319	0.7
4.93722E-07	0.04876874	3	-2.325216077	0.153559391	69.615	24.17443232	0
4.99492E-07	0.158744752	85	-1.723296886	0.371951938	17.81024096	7.74136806	0.4
5.07314E-07	0.12820882	74	-1.93328967	0.278126762	23.854	9.985910194	0
5.08780E-07	0.172074038	94	-1.68434778	0.381311733	16.54964895	7.634522652	0.3
5.09719E-07	0.002444161	36	-2.099328143	0.158381459	305.533	62.92273183	0
5.10720E-07	0.187349958	84	-1.584976378	0.400536473	14.19539078	6.911889862	0.2
5.12413E-07	0.014328371	75	-2.353418201	0.129180266	167.381	43.14941148	0
5.22986E-07	0.027897215	39	-2.376066156	0.128146985	113.429	32.94559715	0
5.26933E-07	0.018889169	53	-2.374738531	0.129071437	147.882	39.6916049	0
5.30076E-07	0.086444759	47	-2.170540461	0.210112043	41.69	15.81385399	0
5.31326E-07	0.092535834	63	-2.119109716	0.239276734	37.306	14.97606913	0
5.41062E-07	0.142412853	61	-1.854984828	0.323955412	22.439	9.4031217	0
5.41403E-07	0.098318418	61	-2.117486568	0.220078354	36.471	13.97671304	0
5.45228E-07	0.071245859	56	-2.241210892	0.187757874	50.269	18.60469763	0
5.46210E-07	0.089440989	94	-2.161198011	0.211059968	40.233	14.83964036	0
5.47140E-07	0.18887474	83	-1.591718244	0.40295329	15.03614458	6.949256046	0.4
5.50747E-07	0.092513615	87	-2.132668265	0.227529601	38.957	15.1101114	0
5.55891E-07	0.041245357	79	-2.358015556	0.140884001	87.064	28.91944395	0
5.62946E-07	0.127920307	1	-1.935608969	0.301668399	26.14414414	10.81272738	0.1
5.63912E-07	0.061802322	41	-2.286673673	0.176634746	61.096	21.66772425	0
5.67740E-07	0.073935846	64	-2.241936708	0.17885454	50.633	18.87311595	0
5.73891E-07	0.036132675	51	-2.381969483	0.127099659	100.507	31.59592147	0
5.76137E-07	0.093415537	69	-2.135582306	0.233306332	40.19	15.81980297	0
5.77759E-07	0.136922281	1	-1.891555179	0.317840469	25.21021021	10.53754885	0.1
5.83091E-07	0.118965916	71	-2.009976284	0.275477983	30.95	12.67636345	0
5.86024E-07	0.042663324	28	-2.365750061	0.144936209	91.262	29.73596448	0
5.87869E-07	0.068704733	30	-2.268775213	0.174609937	56.323	20.37085277	0
5.88930E-07	0.151381812	81	-1.835404395	0.321817992	22.28928929	9.451245817	0.1
5.89784E-07	0.121789582	5	-1.985400331	0.287559606	29.799	11.78386433	0

bioRxiv preprint doi: https://doi.org/10.1101/863894; this version posted December 4, 2019. The copyright holder for this preprint (which was not certified by peer review) is the author/funder. All rights reserved. No reuse allowed without permission.

5.92252E-07	0.012728503	89	-2.365315467	0.126212424	195.285	48.73625958	0
5.97764E-07	0.061090506	26	-2.300659524	0.164891714	64.284	22.72980396	0
6.07912E-07	0.064251841	3	-2.292260897	0.170357909	63.575	23.29611736	0
6.10206E-07	0.188284389	45	-1.627234139	0.419554958	16.91291291	7.974874335	0.1
6.11120E-07	0.133549017	28	-1.934261205	0.301857247	27.205	11.16170052	0
6.22853E-07	0.161318926	63	-1.786585267	0.359595657	21.63563564	9.413852166	0.1
6.25570E-07	0.105957438	85	-2.08558759	0.258754248	37.698	15.06823971	0
6.27399E-07	0.021757202	56	-2.39269476	0.124485746	150.373	41.96442403	0
6.29198E-07	0.068921262	90	-2.268622756	0.182335149	59.777	21.2884586	0
6.31635E-07	0.10812276	39	-2.074949967	0.271997634	37.18018018	14.75027827	0.1
6.32878E-07	0.126549014	23	-1.967960893	0.29350933	29.778	12.50388192	0
6.33823E-07	0.178907936	73	-1.671331584	0.389386425	18.62725451	8.126466455	0.2
6.34670E-07	0.154019599	35	-1.821776121	0.367887564	23.32	10.25567057	0
6.41006E-07	0.003459179	72	-2.195076763	0.160541996	332.256	69.47318178	0
6.46468E-07	0.185159712	30	-1.67006804	0.386386813	18.021	8.141058643	0
6.48995E-07	0.073932404	98	-2.257821508	0.188034544	57.549	21.1703515	0
6.49178E-07	0.005010425	31	-2.26484028	0.133943974	298.541	65.20969731	0
6.49894E-07	0.11317488	43	-2.057983013	0.253372833	35.365	14.2420016	0
6.51568E-07	0.063328497	14	-2.306086825	0.170116923	68.583	24.40845927	0
6.54198E-07	0.174952414	5	-1.735161693	0.36212374	19.96693387	9.099136865	0.2
6.56364E-07	0.06533232	43	-2.309508619	0.163992778	66.057	22.59646767	0
6.56444E-07	0.12333492	71	-2.010133434	0.259923441	32.09309309	13.0049452	0.1
6.57346E-07	0.056927165	57	-2.33082492	0.157865604	74.947	26.47869544	0
6.63547E-07	0.027365637	8	-2.395972024	0.129348737	137.284	40.18300658	0
6.73692E-07	0.067769351	19	-2.282983501	0.176197349	64.356	22.75044718	0
6.74776E-07	0.196447317	43	-1.613491562	0.40610367	17.39418255	8.310012726	0.3
6.78815E-07	0.17252288	2	-1.739164739	0.386092426	20.58458458	8.968359133	0.1
6.90168E-07	0.065720653	72	-2.303813215	0.185377957	68.618	24.48807346	0
6.93034E-07	0.172551217	87	-1.726582668	0.414998201	21.269	9.367517782	0
7.00209E-07	0.112848824	13	-2.072358438	0.262180829	38.486	15.41484419	0
7.09381E-07	0.160081838	6	-1.815992771	0.367069638	24.058	10.77073092	0
7.15598E-07	0.165907051	83	-1.796755044	0.35085572	23.47895792	10.46928248	0.2
7.18303E-07	0.172914761	12	-1.752973161	0.37337729	22.842	10.02544491	0
7.23038E-07	0.04067889	20	-2.399535512	0.134623914	109.438	35.41327797	0
7.23864E-07	0.03023938	10	-2.413917369	0.122199938	139.245	40.93830627	0
7.27150E-07	0.068464767	65	-2.305793295	0.173574978	68.654	24.55596219	0
7.28669E-07	0.170839024	21	-1.782422594	0.346860099	22.904	10.1905167	0
7.32970E-07	0.029525725	27	-2.411539847	0.123930862	140.514	41.50091722	0
7.35494E-07	0.109352402	57	-2.129564421	0.262158095	42.374	16.45627336	0
7.37999E-07	0.064538844	81	-2.312447822	0.166700053	74.775	26.43901277	0
7.38471E-07	0.08708861	88	-2.217086612	0.20560124	53.985	20.49851126	0
7.40200E-07	0.007122198	86	-2.31763108	0.131482564	287.851	66.02461699	0
7.43858E-07	0.11097448	35	-2.093753998	0.262317469	40.736	16.4614484	0
7.45283E-07	0.170784282	98	-1.769886522	0.3851698	23.35535536	9.907834234	0.1
7.45887E-07	0.133740643	95	-1.963543268	0.307146824	32.626	13.65622996	0
7.46177E-07	0.11206069	49	-2.089201067	0.270413636	40.621	16.06497564	0
7.48587E-07	0.186016318	11	-1.686835983	0.397049695	20.669	9.039311265	0
7.54685E-07	0.050743669	12	-2.368816153	0.143035592	94.978	31.31974525	0
7.56554E-07	0.083511943	5	-2.225624981	0.214401708	58.178	21.59436576	0
7.57696E-07	0.118715895	99	-2.052701247	0.273423057	37.426	14.9596228	0
7.66015E-07	0.103301166	9	-2.142747128	0.236139051	46.152	17.97325607	0
7.67139E-07	0.122464078	44	-2.039258757	0.295693826	38.223	15.98138529	0

bioRxiv preprint doi: https://doi.org/10.1101/863894; this version posted December 4, 2019. The copyright holder for this preprint (which was not certified by peer review) is the author/funder. All rights reserved. No reuse allowed without permission.

7.70460E-07	0.124639136	50	-2.020184672	0.289891967	36.467	14.2701278	0
7.73181E-07	0.109563451	56	-2.124596041	0.265118401	43.723	16.6645125	0
7.73734E-07	0.124131001	5	-2.039788628	0.275645329	37.339	14.8165316	0
7.78532E-07	0.157891765	88	-1.866056127	0.31694272	27.212	11.84699993	0
7.81036E-07	0.113441656	88	-2.104894273	0.242571695	42.251	17.24341423	0
7.83887E-07	0.071466447	8	-2.300577909	0.174653556	70.637	25.09424141	0
7.87408E-07	0.186779623	60	-1.687090532	0.417185199	21.37037037	9.599858203	0.1
7.88540E-07	0.119359156	87	-2.073129193	0.268431024	40.545	16.40503277	0
7.91644E-07	0.165678778	3	-1.809017429	0.369616887	26.101	11.59565687	0
7.91907E-07	0.009790842	64	-2.362107843	0.122243822	263.733	62.03558757	0
7.95075E-07	0.056661637	65	-2.359263741	0.147817899	88.329	30.44167299	0
8.02179E-07	0.118936536	93	-2.065181003	0.277919237	40.489	16.40405352	0
8.03831E-07	0.037715098	27	-2.408939246	0.126806834	124.749	38.86672898	0
8.03971E-07	0.126911162	96	-2.038649188	0.293079635	37.673	14.9958977	0
8.11561E-07	0.057371531	47	-2.359531602	0.157725104	90.97	30.8348486	0
8.23590E-07	0.047100156	17	-2.392813941	0.136277983	110.282	34.90161312	0
8.24378E-07	0.126318938	38	-2.04625646	0.276387324	38.651	15.02027988	0
8.26177E-07	0.119302398	1	-2.073597824	0.274128725	41.908	16.18287433	0
8.31952E-07	0.146472046	42	-1.952159634	0.307756778	32.588	14.11082462	0
8.33841E-07	0.096896669	78	-2.202043903	0.214839821	54.368	20.76935102	0
8.38476E-07	0.002551945	68	-2.226928671	0.141982707	390.475	83.64899599	0
8.42650E-07	0.127731742	62	-2.035720753	0.29161473	38.438	15.94115041	0
8.42714E-07	0.001324957	32	-2.079184	0.160879099	458.899	98.29746279	0
8.43452E-07	0.09768117	61	-2.173849678	0.233342268	53.819	20.21323363	0
8.43739E-07	0.067761497	6	-2.32000126	0.176019352	78.947	28.20400072	0
8.45572E-07	0.096051999	25	-2.178944854	0.231792045	54.742	21.13433453	0
8.45649E-07	0.183461131	6	-1.729375924	0.383622783	24.14714715	10.73796896	0.1
8.46633E-07	0.087285589	4	-2.223955615	0.221679003	59.829	22.29041547	0
8.47860E-07	0.10837639	53	-2.122915155	0.251857677	48.35	18.69521359	0
8.50572E-07	0.151922227	37	-1.892116848	0.340573934	31.512	13.80660996	0
8.58158E-07	0.041572711	27	-2.412564388	0.13991195	122.952	37.92827771	0
8.60427E-07	0.076306496	11	-2.29049708	0.179318653	70.689	24.50376938	0
8.63109E-07	0.018727661	82	-2.41929724	0.11599439	209.869	57.66908672	0
8.67748E-07	0.013888134	43	-2.400844977	0.118750513	242.481	59.70387082	0
8.72738E-07	0.151899147	57	-1.908351221	0.333381894	32.321	13.70298255	0
8.79088E-07	0.188572366	20	-1.731098666	0.392420045	23.61661662	10.46514226	0.1
8.90965E-07	0.076500045	30	-2.279598181	0.19632722	72.923	26.49900504	0
8.93050E-07	0.189576839	94	-1.721203809	0.426115355	23.83	10.84853865	0
8.94638E-07	0.088764927	77	-2.229402964	0.213832092	61.753	23.17703963	0
8.95009E-07	0.168161572	30	-1.821728785	0.354682282	28.7987988	12.21896742	0.1
8.95196E-07	0.071280684	69	-2.31169661	0.168400319	79.715	27.37299867	0
1.02549E-08	0.166621462	95	-0.927770559	0.303715992	2.095238095	0.297101757	95.8
1.06950E-08	0.040927772	48	-1.258643589	0.237590368	3.196638655	1.430778365	40.5
1.08510E-08	0.044886013	80	-1.257029637	0.211540237	3.107407407	1.239254646	46
1.10037E-08	0.027449551	44	-1.349544288	0.264949911	4.158653846	2.006325044	16.8
1.10591E-08	0.18920789	62	-0.989228572	0.329183214	2.136363636	0.408679615	95.6
1.13372E-08	0.071016741	54	-1.176759065	0.19201822	2.513368984	0.791091748	62.6
1.13524E-08	0.100426938	67	-1.116350232	0.214595091	2.381188119	0.682578207	79.8
1.18474E-08	0.186101365	97	-0.938338761	0.276544438	2.055555556	0.231212282	94.6
1.19672E-08	0.025621418	80	-1.374937961	0.260214865	4.498281787	2.085953301	12.7
1.31692E-08	0.019304788	75	-1.47088918	0.276639827	6.058762887	2.82982248	3
1.37567E-08	0.191421556	45	-0.891193972	0.327302406	2.229508197	0.588598409	93.9

bioRxiv preprint doi: https://doi.org/10.1101/863894; this version posted December 4, 2019. The copyright holder for this preprint (which was not certified by peer review) is the author/funder. All rights reserved. No reuse allowed without permission.

1.38273E-08	0.002268162	93	-1.232773757	0.461863392	19.673	6.084002473	0
1.38322E-08	0.004473975	55	-1.398755614	0.367019519	15.665	5.113210334	0
1.39104E-08	0.097980034	45	-1.135839726	0.220761062	2.526717557	0.725329829	73.8
1.42461E-08	0.157215948	94	-0.955310389	0.294724987	2.2	0.447213595	89.5
1.49193E-08	0.032895211	3	-1.393375055	0.259908002	4.393764434	2.127368134	13.4
1.50476E-08	0.174141262	35	-1.00275352	0.235382276	2.295238095	0.517460692	89.5
1.51772E-08	0.178423798	65	-0.950406587	0.317505773	2.2	0.451946146	90.5
1.52825E-08	0.160833498	96	-0.988483119	0.33707976	2.170212766	0.377834744	90.6
1.58587E-08	0.028057542	54	-1.460617053	0.265502247	5.25958379	2.494177132	8.7
1.63525E-08	0.104537563	51	-1.136497959	0.230661079	2.528239203	0.814473177	69.9
1.70225E-08	0.134994325	99	-1.063572288	0.257651468	2.380952381	0.745808959	81.1
1.72272E-08	0.162494036	91	-1.005188644	0.299550167	2.276785714	0.54043395	88.8
1.77815E-08	0.06838154	25	-1.235681601	0.225890137	2.978533095	1.189667582	44.1
1.82548E-08	0.001912839	99	-1.309060885	0.42393027	24.852	7.278122496	0
1.82589E-08	0.194236652	81	-0.965604974	0.336085499	2.220930233	0.470323113	91.4
1.86388E-08	0.168700576	34	-1.019028473	0.267958198	2.345588235	0.6131724	86.4
1.87695E-08	0.04253625	20	-1.397551404	0.247532211	4.240143369	1.922770623	16.3
1.93798E-08	0.029317604	67	-1.518148596	0.267990532	6.057894737	2.760517924	5
2.00498E-08	0.147561911	2	-1.041229389	0.250834505	2.398989899	0.717722703	80.2
2.01275E-08	0.119226668	90	-1.107970939	0.260777195	2.53125	0.799073719	68
2.06463E-08	0.033862157	66	-1.498791879	0.281356725	5.629669157	2.613756997	6.3
2.07996E-08	0.08871058	37	-1.20025501	0.230868452	2.815286624	1.036493615	52.9
2.08299E-08	0.044935262	79	-1.40027667	0.258072736	4.409038239	2.135928837	13.7
2.10308E-08	0.188900915	92	-0.930119822	0.313707961	2.295454545	0.534870126	86.8
2.13643E-08	0.186701684	98	-1.022212528	0.290788563	2.348484848	0.641858567	86.8
2.17089E-08	0.126026928	68	-1.097393858	0.273962162	2.605015674	0.961903209	68.1
2.17641E-08	0.019118405	96	-1.661553305	0.260471933	9.518108652	4.004299558	0.6
2.19014E-08	0.088611417	59	-1.19748045	0.239604912	2.880324544	1.106098347	50.7
2.27139E-08	0.04778282	6	-1.411357093	0.251557644	4.427710843	2.095190267	17
2.28218E-08	0.193667433	13	-0.96211986	0.30454337	2.201680672	0.461754795	88.1
2.33544E-08	0.190849318	66	-0.977355022	0.313655215	2.322368421	0.636650732	84.8
2.36558E-08	0.001948288	88	-1.374743654	0.411292592	30.966	8.485803018	0
2.42326E-08	0.108126355	4	-1.159389608	0.245092304	2.777272727	1.088532823	56
2.42992E-08	0.142113581	61	-1.065484424	0.233305221	2.443661972	0.728274478	71.6
2.43615E-08	0.158688121	81	-1.068279613	0.279633649	2.517073171	0.770759251	79.5
2.43992E-08	0.00658896	63	-1.694715431	0.28573051	20.76	6.63041193	0
2.49798E-08	0.010398879	45	-1.748196946	0.265568396	17.148	6.033780117	0
2.51393E-08	0.186037772	52	-0.984606054	0.315367101	2.357575758	0.68031122	83.5
2.52103E-08	0.126946612	66	-1.122561726	0.261626974	2.653521127	0.930316602	64.5
2.59100E-08	0.116103656	74	-1.112509918	0.269557827	2.72361809	1.025614014	60.2
2.61081E-08	0.162699277	46	-1.048846153	0.247566932	2.408071749	0.728646378	77.7
2.63367E-08	0.077065189	13	-1.294867779	0.253340497	3.54294032	1.536002944	31.3
2.63809E-08	0.06712947	27	-1.327597687	0.257203152	3.785620915	1.771960871	23.5
2.69864E-08	0.196584834	30	-0.947872541	0.320109436	2.347058824	0.664053936	83
2.71456E-08	0.193349643	16	-0.946533214	0.339147232	2.388888889	0.654924525	82
2.72271E-08	0.179197088	60	-0.99816553	0.30528566	2.391509434	0.690163512	78.8
2.72913E-08	0.051432378	32	-1.453762469	0.260203136	4.895761741	2.237994043	12.7
2.74122E-08	0.126417189	93	-1.119262301	0.273767692	2.722527473	1.037818323	63.6
2.74777E-08	0.187174034	43	-0.939425824	0.344707126	2.434782609	0.772538896	81.6
2.77261E-08	0.135177669	48	-1.096222267	0.274659883	2.626740947	0.933521127	64.1
2.77473E-08	0.011572525	50	-1.787263772	0.245301687	16.83583584	5.907187724	0.1
2.78436E-08	0.158181546	29	-1.075676761	0.28069892	2.625	0.914344911	73.6

bioRxiv preprint doi: https://doi.org/10.1101/863894; this version posted December 4, 2019. The copyright holder for this preprint (which was not certified by peer review) is the author/funder. All rights reserved. No reuse allowed without permission.

2.79716E-08	0.121370404	23	-1.140570717	0.22730336	2.767494357	1.066830124	55.7
2.80729E-08	0.124909106	73	-1.119453462	0.278057272	2.762626263	1.071715611	60.4
2.82604E-08	0.181244541	30	-0.979477082	0.321192902	2.418719212	0.729196177	79.7
2.86772E-08	0.018544266	96	-1.767353907	0.241837272	12.40540541	4.853444412	0.1
2.93195E-08	0.130182068	74	-1.09413657	0.290354767	2.743529412	1.005931355	57.5
3.01743E-08	0.18749573	90	-0.984159067	0.285103658	2.372641509	0.658741155	78.8
3.03145E-08	0.038624241	15	-1.591359269	0.253253933	6.70880829	3.20256237	3.5
3.03352E-08	0.072671652	78	-1.313701349	0.262304542	3.765306122	1.79996322	21.6
3.04411E-08	0.068350278	19	-1.356203388	0.2564287	4.048689139	1.92779055	19.9
3.10588E-08	0.024551968	14	-1.740643367	0.245955077	10.40080564	4.45321551	0.7
3.10593E-08	0.109796989	53	-1.173573286	0.272641215	3.001988072	1.264752005	49.7
3.15457E-08	0.006028588	66	-1.743420009	0.278227625	27.554	7.935619576	0
3.16380E-08	0.03873084	24	-1.599565843	0.25658156	6.845435685	3.172108771	3.6
3.19440E-08	0.126001308	32	-1.150032042	0.257219056	2.902953586	1.138910002	52.6
3.28659E-08	0.188181744	55	-1.012516885	0.290534947	2.445544554	0.785126	79.8
3.28880E-08	0.070431639	45	-1.380510201	0.255350269	4.323636364	2.009863146	17.5
3.29551E-08	0.128145353	22	-1.154887402	0.281660236	2.969565217	1.229249477	54
3.32757E-08	0.15603905	62	-1.056789878	0.289017561	2.611594203	0.964415752	65.5
3.34054E-08	0.131182663	33	-1.142894011	0.298182441	2.887417219	1.178023579	54.7
3.40177E-08	0.075036148	81	-1.338646579	0.271325031	4.005025126	1.949029721	20.4
3.46501E-08	0.037579753	47	-1.641431633	0.262216759	7.686734694	3.578797447	2
3.54171E-08	0.13890189	18	-1.106733977	0.270906155	2.764150943	1.065707785	57.6
3.58636E-08	0.03356998	77	-1.707681451	0.256625339	9.06612411	3.989127527	1.7
3.60594E-08	0.077295303	63	-1.360822456	0.254736297	4.15776699	1.963051872	17.6
3.64318E-08	0.135068725	40	-1.134055041	0.283041339	2.919354839	1.183023172	50.4
3.67460E-08	0.088118733	24	-1.306619464	0.277618495	3.779548473	1.792198314	24.7
3.74177E-08	0.085571195	24	-1.314211951	0.288079899	3.898832685	1.792520155	22.9
3.79671E-08	0.097927423	31	-1.277687544	0.280236214	3.627737226	1.626746921	31.5
3.83399E-08	0.18967709	84	-0.948242067	0.347297603	2.518394649	0.8286984	70.1
3.87822E-08	0.160174614	45	-1.07006409	0.3153692	2.712328767	0.97326137	63.5
3.88599E-08	0.074314286	71	-1.392087492	0.279256515	4.544273908	2.124964116	15.3
3.97460E-08	0.121794102	59	-1.176261446	0.263746461	3.086805556	1.291887545	42.4
3.98361E-08	0.110882519	14	-1.223632301	0.272236659	3.368499257	1.520990134	32.7
4.00437E-08	0.007419299	65	-1.846489668	0.252321243	31.474	8.789230602	0
4.00787E-08	0.179253021	81	-1.034597282	0.316023444	2.618902439	0.897435703	67.2
4.06806E-08	0.004447736	33	-1.728623338	0.282180432	40.536	10.68198525	0
4.10283E-08	0.179458796	67	-1.035383639	0.326309415	2.576923077	0.841258066	66.2
4.17174E-08	0.064628208	43	-1.488539862	0.278977912	5.521546961	2.765109304	9.5
4.18112E-08	0.014176559	58	-1.911656544	0.215369676	22.101	7.368520482	0
4.21990E-08	0.069601105	87	-1.448272612	0.273257538	5.067114094	2.59510547	10.6
4.22649E-08	0.059863422	3	-1.52545127	0.273099346	5.825531915	2.751587253	6
4.22991E-08	0.068692159	83	-1.464700005	0.271343289	5.1171875	2.455570639	10.4
4.30696E-08	0.093657618	49	-1.319643736	0.268975063	4.039042821	2.047909669	20.6
4.30767E-08	0.120789975	19	-1.204555362	0.26835306	3.321821036	1.396889338	36.3
4.40754E-08	0.150367728	4	-1.116256619	0.290956678	3.004106776	1.247212354	51.3
4.41865E-08	0.174184304	47	-1.065990165	0.309784824	2.800970874	1.091528551	58.8
4.42550E-08	0.048952082	28	-1.632507696	0.271695922	7.392820513	3.559489983	2.5
4.45005E-08	0.00605235	67	-1.838727553	0.262381873	37.079	10.21661089	0
4.51102E-08	0.116337226	30	-1.225835771	0.278870589	3.515151515	1.584661151	34
4.51624E-08	0.008590777	67	-1.902690269	0.239763927	31.809	9.51015047	0
4.52507E-08	0.072360345	27	-1.473201546	0.27838139	5.336225597	2.591175634	7.8
4.52644E-08	0.049148661	7	-1.640454573	0.275062185	7.625514403	3.512474055	2.8

bioRxiv preprint doi: https://doi.org/10.1101/863894; this version posted December 4, 2019. The copyright holder for this preprint (which was not certified by peer review) is the author/funder. All rights reserved. No reuse allowed without permission.

4.58375E-08	0.082761083	11	-1.390266488	0.263988306	4.568469505	2.192145611	13.1
4.59814E-08	0.015692463	76	-1.939526346	0.21191459	22.119	7.431693553	0
4.65201E-08	0.087850088	88	-1.375365351	0.274626443	4.430094787	2.148926072	15.6
4.69712E-08	0.169363729	77	-1.056946782	0.316878342	2.922727273	1.247660889	56
4.74198E-08	0.15336794	44	-1.101334501	0.312214703	3.005882353	1.361108956	49
4.77424E-08	0.141501597	52	-1.139694211	0.331548142	3.19343696	1.455412913	42.1
4.77553E-08	0.1518446	82	-1.121040941	0.306511403	3.082568807	1.282865304	45.5
4.79167E-08	0.179497246	48	-1.054439002	0.304803988	2.708860759	0.994297175	60.5
4.80844E-08	0.145199405	61	-1.115385886	0.309429088	3.070143885	1.322204267	44.4
4.93696E-08	0.056948265	49	-1.605599545	0.273239165	7.047131148	3.42147546	2.4
4.95222E-08	0.125806707	84	-1.213863937	0.259113039	3.459541985	1.480080719	34.5
4.95710E-08	0.121119899	73	-1.232531223	0.291127904	3.631954351	1.657469768	29.9
4.97218E-08	0.106983586	29	-1.276708714	0.311563474	3.909214092	1.897980554	26.2
5.00838E-08	0.01152962	31	-1.965089939	0.211308235	28.862	8.914730979	0
5.11168E-08	0.168721148	63	-1.068644978	0.331325362	2.915019763	1.152995109	49.4
5.14290E-08	0.163176623	86	-1.104035862	0.296823345	3.005928854	1.233992324	49.4
5.15830E-08	0.087953779	20	-1.376949878	0.286049984	4.653758542	2.228339958	12.2
5.17548E-08	0.161152842	41	-1.090584051	0.297859921	3.024048096	1.187037945	50.1
5.19361E-08	0.062704661	41	-1.595235379	0.282411658	6.860294118	3.356243944	4.8
5.28199E-08	0.042245061	71	-1.779328133	0.247690781	10.45975855	4.487746587	0.6
5.28255E-08	0.063306001	46	-1.567188051	0.281668395	6.61105318	3.207168842	4.1
5.31820E-08	0.008935906	60	-1.948120994	0.231650327	36.118	10.16047791	0
5.33833E-08	0.196059525	42	-0.9888226	0.339468613	2.664160401	0.949738782	60.1
5.36643E-08	0.106108984	82	-1.321821568	0.283392556	4.155927835	1.948409685	22.4
5.37567E-08	0.115271647	96	-1.262042197	0.291454253	3.822768435	1.731571838	22.7
5.37605E-08	0.136818281	26	-1.174428789	0.308828459	3.341732283	1.451010794	36.5
5.42478E-08	0.007267228	87	-1.902644506	0.239456324	40.917	10.80772492	0
5.45313E-08	0.122548245	11	-1.235431792	0.279289648	3.67798913	1.622412508	26.4
5.47603E-08	0.109345728	20	-1.299795208	0.296287224	4.131611316	1.954821496	18.7
5.56244E-08	0.10416775	53	-1.334503008	0.291461337	4.369512195	2.121187323	18
5.56793E-08	0.12543903	51	-1.226467123	0.303297667	3.671724138	1.825944978	27.5
5.57216E-08	0.180434003	80	-1.082790968	0.314082881	3.078947368	1.257771825	50.6
5.58493E-08	0.193865959	78	-1.0217415	0.347692376	2.826506024	1.076212308	58.5
5.60914E-08	0.058138095	29	-1.667646791	0.264036245	8.047082907	3.731489037	2.3
5.61151E-08	0.112464925	61	-1.305162748	0.286586333	4.119791667	1.918475046	23.2
5.64214E-08	0.195214354	54	-1.000697513	0.322795056	2.84057971	1.106308414	58.6
5.64275E-08	0.187407629	14	-1.026662064	0.346304436	2.915367483	1.148352823	55.1
5.66711E-08	0.18264967	63	-1.037419448	0.321467929	2.884090909	1.18368622	56
5.69467E-08	0.095471112	95	-1.386375075	0.297169207	4.825934579	2.399577022	14.4
5.77445E-08	0.035818002	73	-1.874570294	0.223807816	13.02802803	5.214940693	0.1
5.80649E-08	0.146920977	22	-1.163898799	0.314599189	3.381789137	1.532450271	37.4
5.82768E-08	0.13321176	78	-1.212145201	0.291306829	3.552407932	1.649655415	29.4
5.83021E-08	0.051742495	9	-1.716831162	0.264563631	9.013184584	4.178119048	1.4
5.88793E-08	0.025214899	55	-1.97655638	0.209226376	19.125	6.973378163	0
5.97397E-08	0.151678629	64	-1.141115748	0.323160391	3.373417722	1.486267524	36.8
5.98344E-08	0.041260736	11	-1.832199046	0.245698481	11.90562249	4.958838464	0.4
6.04012E-08	0.151567184	32	-1.157430252	0.290811915	3.322033898	1.421665969	35.1
6.04017E-08	0.046380679	38	-1.791959762	0.258017848	10.77194753	4.819411522	0.9
6.04703E-08	0.171901895	29	-1.113354796	0.300565883	3.130208333	1.256104658	42.4
6.08165E-08	0.078767198	58	-1.514779552	0.29173394	6.097430407	3.021915988	6.6
6.08671E-08	0.080094909	40	-1.51341542	0.290154984	6.069222577	2.962541649	6.1
6.09768E-08	0.04038015	95	-1.858603574	0.235942864	12.66566567	5.250282208	0.1

bioRxiv preprint doi: https://doi.org/10.1101/863894; this version posted December 4, 2019. The copyright holder for this preprint (which was not certified by peer review) is the author/funder. All rights reserved. No reuse allowed without permission.

6.16821E-08	0.093311023	70	-1.413053499	0.305851606	5.192784667	2.539092509	11.3
6.18358E-08	0.003105391	23	-1.757031883	0.284076314	61.184	15.78928261	0
6.19557E-08	0.000680834	10	-1.472204287	0.370760764	78.733	18.19947614	0
6.25196E-08	0.043548086	61	-1.847056048	0.240738027	11.91247485	5.026354042	0.6
6.26388E-08	0.006197232	3	-1.910359979	0.241603025	49.656	12.78542651	0
6.28144E-08	0.089991688	42	-1.430386712	0.287536753	5.266015201	2.545205697	7.9
6.29269E-08	0.062816499	28	-1.655222565	0.266685946	8.060762101	3.726115005	2.9
6.29490E-08	0.115705576	38	-1.299440858	0.300059441	4.261239368	2.044169662	17.7
6.30087E-08	0.02833647	39	-1.97211339	0.213786015	18.08508509	6.827077394	0.1
6.32787E-08	0.11565336	8	-1.298228507	0.300252073	4.216381418	2.03539683	18.2
6.34922E-08	0.177816587	63	-1.065888142	0.327278154	3.118299445	1.308397971	45.9
6.37770E-08	0.091894077	37	-1.425144197	0.297130513	5.27795874	2.696382956	7.9
6.39081E-08	0.136685745	87	-1.213213947	0.30062682	3.742587601	1.715152064	25.8
6.44031E-08	0.062268	87	-1.675588309	0.262221322	8.286004057	3.841708965	1.4
6.51204E-08	0.182882459	9	-1.017862616	0.369157437	3.005545287	1.197979289	45.9
6.52500E-08	0.055291347	46	-1.729548834	0.276368097	9.520812183	4.549839557	1.5
6.54777E-08	0.018066283	90	-2.031396988	0.192812536	27.293	8.980857799	0
6.59931E-08	0.107429777	38	-1.368804037	0.30531698	4.791860465	2.426028585	14
6.62527E-08	0.103102162	94	-1.380413344	0.306068572	4.863945578	2.449414086	11.8
6.63110E-08	0.168995134	48	-1.119446729	0.314576364	3.191558442	1.337025034	38.4
6.65924E-08	0.156218456	91	-1.14480705	0.32362419	3.484210526	1.569707694	33.5
6.70064E-08	0.107908052	22	-1.351492211	0.308453316	4.710801394	2.351889282	13.9
6.78114E-08	0.139843505	17	-1.212771296	0.323831975	3.74796748	1.682023218	26.2
6.78407E-08	0.172280952	39	-1.095421821	0.366439467	3.274873524	1.420289521	40.7
6.84194E-08	0.006145635	27	-1.946685872	0.236363442	54.12	13.78069329	0
6.84434E-08	0.12504925	92	-1.292133108	0.312171698	4.207286432	2.007782888	20.4
6.87551E-08	0.156191324	37	-1.119010364	0.334869372	3.391629297	1.525920319	33.1
6.88514E-08	0.046376509	52	-1.836189957	0.241212578	12.01603206	5.183662272	0.2
6.89897E-08	0.109093	83	-1.358025461	0.312075186	4.790993072	2.357908779	13.4
6.90035E-08	0.038231201	30	-1.906839032	0.238527403	14.6002004	5.859392237	0.2
7.10289E-08	0.011504202	9	-2.037323738	0.200623867	38.597	11.53002743	0
7.16371E-08	0.119795949	33	-1.316158395	0.313163254	4.464670659	2.129981194	16.5
7.19062E-08	0.108944477	12	-1.380574391	0.288661169	4.992081448	2.469965582	11.6
7.21496E-08	0.098247163	75	-1.436293783	0.308634183	5.46961326	2.786546052	9.5
7.25245E-08	0.103848526	67	-1.426490338	0.302543919	5.431263858	2.54574973	9.8
7.27304E-08	0.117376649	22	-1.349979489	0.289068135	4.754022989	2.19250762	13
7.32176E-08	0.146257167	77	-1.200394421	0.32146923	3.733695652	1.815205746	26.4
7.39357E-08	0.067156525	6	-1.681634223	0.279895496	8.593462717	4.078749127	2.1
7.41321E-08	0.053917111	80	-1.797485041	0.250298879	10.92978937	4.867633994	0.3
7.47834E-08	0.01056615	62	-2.041916749	0.197098565	42.509	12.23558861	0
7.53146E-08	0.035572741	85	-1.977216193	0.209541238	17.444	6.943707877	0
7.57802E-08	0.10716773	18	-1.406796573	0.31238153	5.28443449	2.702712812	10.7
7.64065E-08	0.138503474	65	-1.240604605	0.331338091	4.090676884	2.014195765	21.7
7.64381E-08	0.196662457	81	-1.038466995	0.350915754	3.114840989	1.288159375	43.4
7.64884E-08	0.104148309	41	-1.437612716	0.291200144	5.499454744	2.621970018	8.3
7.66837E-08	0.035334821	34	-1.982120303	0.207827013	17.65465465	6.702514697	0.1
7.70067E-08	0.104346935	4	-1.434300125	0.305645228	5.468271335	2.664845554	8.6
7.70446E-08	0.119738701	48	-1.347977488	0.287615347	4.806146572	2.348412038	15.4
7.72469E-08	0.107084332	87	-1.408349231	0.313113278	5.424342105	2.700323111	8.8
7.74814E-08	0.104165302	9	-1.429079279	0.318819512	5.551155116	2.726293753	9.1
7.75143E-08	0.19806486	69	-1.045020452	0.33264489	3.119565217	1.290836541	44.8
7.78493E-08	0.15580692	62	-1.176273047	0.347146339	3.754143646	1.691340556	27.6

bioRxiv preprint doi: https://doi.org/10.1101/863894; this version posted December 4, 2019. The copyright holder for this preprint (which was not certified by peer review) is the author/funder. All rights reserved. No reuse allowed without permission.

7.81855E-08	0.068335055	67	-1.709492144	0.271330355	9.195519348	4.18828767	1.8
7.94475E-08	0.141996715	54	-1.232695038	0.327331097	4.045278137	1.959900886	22.7
7.96747E-08	0.05179033	8	-1.857153814	0.23273021	12.50100402	5.351841743	0.4
7.98109E-08	0.171308257	61	-1.111898946	0.351002857	3.480406386	1.60304284	31.1
7.98632E-08	0.015347036	60	-2.086089792	0.182644749	38.337	11.27086791	0
8.01717E-08	0.029186794	35	-2.041032616	0.183033598	21.92592593	7.99752708	0.1
8.02683E-08	0.077663736	31	-1.637813272	0.27513677	7.854657114	3.883730423	2.3
8.13490E-08	0.062851419	34	-1.761976417	0.258065989	10.15656566	4.642174049	1
8.13954E-08	0.082687839	58	-1.59664563	0.284604228	7.356701031	3.521800225	3
8.27291E-08	0.043498562	10	-1.930263091	0.226905057	15.218	6.20201104	0
8.31551E-08	0.065013744	32	-1.733910921	0.254109252	9.656565657	4.405074783	1
8.32055E-08	0.198865815	7	-1.057386001	0.360799442	3.336148649	1.514792497	40.8
8.34291E-08	0.04059482	20	-1.961650005	0.21302687	16.272	6.307281332	0
8.36063E-08	0.105020254	73	-1.464206677	0.297449383	5.857451404	2.875278334	7.4
8.38460E-08	0.022189871	68	-2.094246755	0.188941813	29.35	9.70008204	0
8.44043E-08	0.173551287	94	-1.120202835	0.367050897	3.553284672	1.739338917	31.5
8.48633E-08	0.007450883	82	-2.009825318	0.220298767	59.352	15.85128889	0
8.50673E-08	0.038016401	81	-2.002247439	0.203001912	18.04	6.680646004	0
8.52202E-08	0.101056905	39	-1.482953891	0.304604221	6.034151547	3.054509618	6.3
8.53627E-08	0.068402003	95	-1.743708689	0.26522379	9.977732794	4.706535812	1.2
8.60217E-08	0.150985712	16	-1.202945275	0.341059198	4.100250627	2.01000632	20.2
8.70011E-08	0.160138506	29	-1.201880229	0.326978693	3.853887399	1.83591088	25.4
8.70292E-08	0.060189765	80	-1.806914909	0.258185685	11.13622603	4.816701739	0.9
8.77588E-08	0.022669986	70	-2.095047571	0.184581303	29.638	9.70026036	0
8.78073E-08	0.048159959	26	-1.908398816	0.226948388	14.48348348	5.882745181	0.1
8.82687E-08	0.011916842	60	-2.099889315	0.187705653	47.196	13.15022861	0
8.85433E-08	0.003956779	87	-1.906430565	0.239726704	76.384	18.27053246	0
8.87385E-08	0.104898223	9	-1.4714337	0.306510486	6.021164021	2.959396254	5.5
8.90021E-08	0.055814096	5	-1.855867407	0.24928679	12.59638554	5.346839294	0.4
8.96809E-08	0.155377217	63	-1.196451693	0.352137991	4.075255102	1.9556252	21.6
8.99073E-08	0.023796868	77	-2.097168783	0.180597954	29.654	9.609090416	0
1.01063E-09	0.16210266	90	-1.145825701	NA	2	NA	99.9
1.01121E-09	0.02783863	96	-1.091958642	0.161187493	2.046511628	0.213082632	95.7
1.04348E-09	0.110131915	50	-0.630464825	NA	2	NA	99.9
1.04485E-09	0.113399701	89	-1.145825701	NA	2	NA	99.9
1.07424E-09	0.055495772	82	-1.047470297	0.16814295	2	0	98.8
1.16816E-09	0.008937843	7	-0.977191086	0.301575353	2.452755906	0.772381643	74.6
1.21365E-09	0.125557871	61	-1.071054154	NA	2	NA	99.9
1.25418E-09	0.09047163	49	-1.02834383	0.302137564	2.166666667	0.389249472	98.8
1.31478E-09	0.039668732	61	-1.120522179	0.138447973	2.125	0.336010753	96.8
1.40847E-09	0.014239514	87	-1.011873337	0.280916267	2.387254902	0.613505083	79.6
1.51991E-09	0.119043647	65	-0.995746611	0.07477731	2	0	99.7
1.52486E-09	0.186840658	79	-1.145825701	0	2	0	99.8
1.62228E-09	0.013049045	11	-1.064911351	0.29785085	2.467857143	0.7613201	72
1.62990E-09	0.090763131	87	-1.145825701	0.076379537	2	0	99.7
1.68352E-09	0.127417494	44	-0.84007784	0.328940047	2	0	99.3
1.76480E-09	0.043105804	9	-1.11251557	0.207585879	2.218181818	0.497806637	94.5
1.81013E-09	0.083598026	91	-1.094679242	0.141481647	2	0	98.7
1.85998E-09	0.025107286	24	-1.089896368	0.21343108	2.291666667	0.601571369	85.6
1.88701E-09	0.032777442	37	-1.109574203	0.195837684	2.26744186	0.540684068	91.4
1.88956E-09	0.022238668	56	-1.088972753	0.216306205	2.353773585	0.625170995	78.8
1.89115E-09	0.050529576	78	-1.119976461	0.214985229	2.125	0.40430377	96

bioRxiv preprint doi: https://doi.org/10.1101/863894; this version posted December 4, 2019. The copyright holder for this preprint (which was not certified by peer review) is the author/funder. All rights reserved. No reuse allowed without permission.

1.90273E-09	0.106539955	82	-0.920335991	0.24306698	2	0	98.7
1.93148E-09	0.021324877	89	-1.092682768	0.207997235	2.327014218	0.570864086	78.9
1.95247E-09	0.112849528	1	-1.006942223	0.224500291	2.090909091	0.301511345	98.9
1.96626E-09	0.117030422	62	-1.339250771	0.123420036	3	0	99.8
1.96692E-09	0.03574858	94	-1.12390884	0.170902929	2.208791209	0.435034699	90.9
2.00049E-09	0.024377374	57	-1.087557527	0.242330438	2.254143646	0.539080453	81.9
2.04593E-09	0.023275372	26	-1.107615277	0.204715163	2.292079208	0.637810803	79.8
2.11450E-09	0.023923197	94	-1.088545706	0.227540295	2.315508021	0.560266002	81.3
2.16334E-09	0.006863784	73	-0.991580847	0.355518766	3.04886562	1.331852752	42.7
2.18700E-09	0.011080759	44	-1.034890037	0.322627879	2.699763593	0.942505957	57.7
2.20747E-09	0.037835737	23	-1.098075992	0.232314364	2.210526316	0.549321751	92.4
2.21115E-09	0.013832197	29	-1.085793598	0.276607108	2.608478803	0.817819008	59.9
2.24444E-09	0.091031659	76	-1.05031108	0.173292801	2	0	98
2.26867E-09	0.036237396	77	-1.125284295	0.179306906	2.188034188	0.434138543	88.3
2.28172E-09	0.000889691	86	-0.455335318	0.695653761	4.59558011	2.068511906	9.5
2.28676E-09	0.024502224	54	-1.093834287	0.191635516	2.288770053	0.510146601	81.3
2.32057E-09	0.042698751	70	-1.107658027	0.188258218	2.240963855	0.508233705	91.7
2.33343E-09	0.121074273	38	-1.072394146	0.122076717	2	0	99.4
2.41399E-09	0.131678674	52	-1.096961473	0.208428635	2.222222222	0.666666667	99.1
2.47316E-09	0.155659682	68	-1.054773253	0.162575919	2	0	99.6
2.50081E-09	0.183060031	59	-0.818197687	0.054008489	2	0	99.8
2.50143E-09	0.009252218	23	-1.048437569	0.332457069	2.979202773	1.191514	42.3
2.51626E-09	0.123918922	39	-1.066741817	0.20780973	2	0	98.9
2.56349E-09	0.1252226	15	-0.998694593	0.102331873	2	0	99.8
2.62040E-09	0.097424746	78	-1.029598257	0.254620082	2.071428571	0.267261242	98.6
2.64796E-09	0.068651967	8	-1.092471575	0.217355616	2.242424242	0.501890366	96.7
2.68883E-09	0.112673204	79	-1.053768259	0.138673972	2	0	98.4
2.77947E-09	0.185757721	46	-0.929551012	0.413875575	2	0	99.8
2.78982E-09	0.04531321	50	-1.145354862	0.170725115	2.295238095	0.553377905	89.5
2.79885E-09	0.143077961	73	-1.096033883	0.146023087	2.125	0.353553391	99.2
2.81030E-09	0.155736687	20	-0.726140245	0.432820529	2	0	99.7
2.87415E-09	0.184450928	36	-1.146227699	0.107259298	2	0	99.6
2.93223E-09	0.175651662	32	-0.886805271	0.206043994	2	0	99.4
2.93377E-09	0.138910089	67	-1.050273973	0.186310394	2	0	98.7
2.94838E-09	0.054018292	97	-1.083275792	0.216980851	2.129411765	0.371234597	91.5
2.95326E-09	0.029782522	83	-1.120805092	0.199546373	2.331730769	0.667067187	79.2
3.05530E-09	0.063345484	66	-1.10044798	0.175957857	2.192307692	0.486623482	94.8
3.09290E-09	0.142877693	81	-0.986419954	0.143515861	2.25	0.46291005	99.2
3.10830E-09	0.199706781	99	-0.925263038	0.070826145	2	0	99.7
3.12244E-09	0.157430658	66	-0.892969234	0.260908084	2	0	99.6
3.23711E-09	0.118960926	96	-1.013065316	0.177162792	2.125	0.341565026	98.4
3.29130E-09	0.153624259	12	-0.962514812	0.276923124	2	0	99.6
3.31882E-09	0.057128617	4	-1.12450918	0.168827861	2.2	0.496798259	90.5
3.33679E-09	0.134054739	16	-0.96682715	0.225471047	2	0	98.9
3.36112E-09	0.090815239	85	-1.112066721	0.170547596	2.205882353	0.41042563	96.6
3.40874E-09	0.142667866	29	-0.926319127	0.238011007	2.076923077	0.277350098	98.7
3.45303E-09	0.116100218	51	-1.044646007	0.186339041	2	0	97.4
3.45651E-09	0.07060834	37	-1.071380657	0.19324928	2.125	0.333711906	94.4
3.47480E-09	0.036088665	87	-1.151943963	0.171793791	2.294642857	0.578204936	77.6
3.48376E-09	0.180788421	35	-1.145825701	0.108016977	2	0	99.8
3.54029E-09	0.195300871	50	-0.848921787	0.419352563	2	0	99.3
3.54969E-09	0.190918855	20	-1.150676802	0.16203972	2.222222222	0.440958552	99.1

bioRxiv preprint doi: https://doi.org/10.1101/863894; this version posted December 4, 2019. The copyright holder for this preprint (which was not certified by peer review) is the author/funder. All rights reserved. No reuse allowed without permission.

3.56340E-09	0.153815397	57	-0.963341718	0.266145164	2.181818182	0.603022689	98.9
3.60466E-09	0.010148286	50	-1.111490862	0.320856386	3.451923077	1.463126473	27.2
3.64423E-09	0.093226633	90	-1.114331816	0.157515526	2.060606061	0.242305842	96.7
3.68285E-09	0.185766621	26	-0.964049503	0.220011664	2.125	0.353553391	99.2
3.71587E-09	0.124887435	96	-0.963318807	0.391565437	2	0	98.9
3.74444E-09	0.040985564	29	-1.134469376	0.17586001	2.317204301	0.580237352	81.4
3.83984E-09	0.156058522	28	-0.941662284	0.352897614	2.111111111	0.333333333	99.1
3.85759E-09	0.106453984	65	-1.059422386	0.216225713	2.041666667	0.204124145	97.6
3.86232E-09	0.140252604	45	-1.019159908	0.226379193	2.090909091	0.301511345	98.9
3.87286E-09	0.145502936	1	-0.999364589	0.29886187	2	0	98.2
3.88632E-09	0.032416763	76	-1.150731117	0.189422701	2.440860215	0.741314683	72.1
3.88713E-09	0.047017897	20	-1.14801296	0.197657482	2.372262774	0.594178861	86.3
3.90645E-09	0.045846424	6	-1.159640492	0.173333038	2.386503067	0.641421583	83.7
3.98044E-09	0.117140945	68	-1.019665069	0.26025968	2.111111111	0.323380833	98.2
4.03000E-09	0.110095979	10	-1.09189299	0.20424468	2.161290323	0.373878251	96.9
4.04572E-09	0.078672153	59	-1.067736191	0.187764467	2.080645161	0.274512211	93.8
4.12910E-09	0.054761298	85	-1.129025389	0.19543459	2.278195489	0.56880235	86.7
4.14914E-09	0.066314677	56	-1.129088865	0.163070482	2.23	0.489382212	90
4.17794E-09	0.0164626	75	-1.164697329	0.256826852	3.111111111	1.251665557	37.9
4.20651E-09	0.087631791	90	-1.060111267	0.19636677	2.140625	0.393082547	93.6
4.21081E-09	0.064123585	21	-1.091860631	0.184766771	2.18	0.435310176	90
4.21166E-09	0.137810585	11	-0.949375807	0.27348087	2.055555556	0.23570226	98.2
4.21670E-09	0.081031449	55	-1.103999122	0.221934433	2.171428571	0.416034717	93
4.22175E-09	0.000272418	2	-0.690351899	0.574334798	7.517694641	2.974408447	1.1
4.23302E-09	0.125799242	99	-1.079104351	0.110959711	2.19047619	0.402373908	97.9
4.24265E-09	0.15514505	25	-1.015750775	0.249887857	2	0	98.6
4.24356E-09	0.100546756	69	-1.077996209	0.173001571	2.171428571	0.452815654	96.5
4.29833E-09	0.024542987	87	-1.183254931	0.235510568	2.779017857	1.01346943	55.2
4.30986E-09	0.098298211	67	-1.06413227	0.14941474	2.054054054	0.229243435	96.3
4.34849E-09	0.183250244	33	-0.924007656	0.360950387	2.4	0.547722558	99.5
4.39763E-09	0.185077495	72	-0.816890897	0.325853019	2.083333333	0.288675135	98.8
4.44240E-09	0.08427651	70	-1.10003641	0.187711485	2.203703704	0.450560642	94.6
4.44845E-09	0.017813951	9	-1.17632356	0.257289987	3.014950166	1.182840041	39.8
4.45830E-09	0.175059041	23	-0.939003085	0.225445017	2.083333333	0.288675135	98.8
4.46223E-09	0.01012841	35	-1.174938511	0.320436358	3.901112485	1.695979885	19.1
4.61902E-09	0.15531995	15	-0.967296223	0.250404309	2.066666667	0.25819889	98.5
4.62164E-09	0.147314766	97	-0.963441291	0.298049124	2.066666667	0.25819889	98.5
4.65305E-09	0.025544625	33	-1.158958286	0.224263791	2.72611465	1.001773735	52.9
4.65635E-09	0.125795606	82	-1.074312293	0.212691774	2.129032258	0.340777101	96.9
4.71245E-09	0.07716111	82	-1.119875884	0.19582935	2.255813953	0.535472227	91.4
4.76454E-09	0.18308596	26	-0.912781971	0.368044164	2	0	98.6
4.79342E-09	0.189459864	1	-0.910850145	0.353987572	2.125	0.353553391	99.2
4.81383E-09	0.045104414	9	-1.156951291	0.167607259	2.376470588	0.669524521	74.5
4.82194E-09	0.002499506	61	-0.874957485	0.551042377	7.516683519	3.228945304	1.1
4.91357E-09	0.014005405	56	-1.199227029	0.3053136	3.652116402	1.645184268	24.4
4.93431E-09	0.005905324	98	-1.17323854	0.390895777	5.510615711	2.454126162	5.8
4.93693E-09	0.196083065	97	-0.990675341	0.312793344	2.125	0.353553391	99.2
4.99813E-09	0.041186126	2	-1.148684672	0.213508447	2.413669065	0.763395553	72.2
5.07083E-09	0.07201194	9	-1.101236057	0.252893583	2.237623762	0.427750274	89.9
5.11498E-09	0.125991801	68	-1.09249882	0.186480789	2.117647059	0.409338408	96.6
5.11716E-09	0.148427856	76	-0.940659832	0.231109065	2.076923077	0.277350098	98.7
5.17769E-09	0.012524331	45	-1.203154545	0.30092923	3.784747847	1.752314048	18.7

bioRxiv preprint doi: https://doi.org/10.1101/863894; this version posted December 4, 2019. The copyright holder for this preprint (which was not certified by peer review) is the author/funder. All rights reserved. No reuse allowed without permission.

5.23359E-09	0.092135821	18	-1.072870612	0.194604565	2.16	0.369074811	92.5
5.29038E-09	0.102290526	95	-1.040962984	0.198739937	2.102040816	0.367701076	95.1
5.31548E-09	0.07914786	25	-1.108323179	0.2058043	2.232876712	0.540589903	92.7
5.33621E-09	0.090563766	34	-1.093543323	0.18512012	2.171052632	0.412735844	92.4
5.38098E-09	0.157451848	38	-0.98324002	0.202145936	2	0	99.1
5.40690E-09	0.1850562	14	-0.800911792	0.303986453	2	0	99.1
5.47559E-09	0.011867331	90	-1.251686516	0.290839207	4.154121864	1.934055869	16.3
5.48605E-09	0.015551803	51	-1.228041601	0.272263023	3.557463672	1.546779523	24.3
5.50414E-09	0.060750666	64	-1.167958256	0.172239781	2.366459627	0.68638037	83.9
5.61863E-09	0.035996163	63	-1.183029093	0.210397859	2.610497238	0.899492178	63.8
5.68850E-09	0.121377724	88	-1.014565598	0.29560012	2.261904762	0.543678699	95.8
5.70741E-09	0.083854371	65	-1.100602574	0.195691176	2.157894737	0.394531488	90.5
5.75030E-09	0.01947594	38	-1.240834241	0.254003225	3.417266187	1.466726445	30.5
5.76505E-09	0.152226504	39	-0.977476766	0.280358507	2.047619048	0.21821789	97.9
5.89865E-09	0.163066009	82	-1.011577341	0.266066545	2.166666667	0.514495755	98.2
5.94085E-09	0.130459109	32	-0.999523754	0.26285265	2.171428571	0.452815654	96.5
5.94539E-09	0.18194444	78	-0.880514104	0.56194322	2.066666667	0.25819889	98.5
5.99600E-09	0.087536784	85	-1.100714669	0.196550605	2.173469388	0.431384972	90.2
6.01210E-09	0.021766128	64	-1.224374271	0.253383362	3.251515152	1.332589345	34
6.07143E-09	0.154425005	98	-0.976111559	0.219431464	2.088235294	0.287902241	96.6
6.08898E-09	0.054544437	75	-1.156228232	0.188529885	2.422413793	0.740315389	76.8
6.10043E-09	0.081826466	73	-1.11798194	0.235621054	2.344537815	0.602775709	88.1
6.10749E-09	0.116399301	41	-1.003188619	0.263561488	2.173076923	0.382004714	94.8
6.14038E-09	0.13420271	4	-0.989565139	0.268687092	2.088235294	0.287902241	96.6
6.17449E-09	0.03962968	86	-1.187697909	0.226122085	2.619302949	0.915724372	62.7
6.18262E-09	0.161237583	10	-1.012258715	0.274510162	2.090909091	0.294244943	97.8
6.18684E-09	0.012842356	44	-1.24529691	0.293635728	4.223760092	1.894623041	13.3
6.19671E-09	0.128649514	16	-1.104318441	0.162947602	2.146341463	0.357839043	95.9
6.20313E-09	0.072950294	19	-1.109074107	0.205247864	2.210144928	0.504764143	86.2
6.32830E-09	0.064723744	36	-1.156063106	0.191197798	2.411428571	0.77451187	82.5
6.34873E-09	0.099776515	91	-1.092183265	0.180593092	2.138297872	0.376773622	90.6
6.34945E-09	0.165175497	93	-0.854390466	0.33572465	2.096774194	0.300537154	96.9
6.38891E-09	0.110258902	97	-1.085744336	0.202904705	2.15	0.40442468	94
6.40015E-09	0.050953377	14	-1.172790902	0.196916738	2.536977492	0.79782923	68.9
6.41778E-09	0.190737532	89	-0.842880338	0.295660345	2	0	99
6.47170E-09	0.060775701	82	-1.163662857	0.178143702	2.450980392	0.757588226	79.6
6.51853E-09	0.004617782	71	-1.210709198	0.399831	7.283076923	3.056932534	2.5
6.60017E-09	0.025945115	24	-1.23999063	0.238003999	3.253968254	1.357640499	37
6.61228E-09	0.155039291	80	-1.077182833	0.198121309	2.192307692	0.491465626	97.4
6.65150E-09	0.089377494	70	-1.122540443	0.212761949	2.292035398	0.677197691	88.7
6.74522E-09	0.028716439	30	-1.229410947	0.225405153	3.053872054	1.223901989	40.6
6.75761E-09	0.181987218	95	-0.90080269	0.283784028	2.041666667	0.204124145	97.6
6.80299E-09	0.035593864	53	-1.218523541	0.218827111	2.816283925	1.026666403	52.1
6.80899E-09	0.139976064	10	-0.92724971	0.31538391	2.051282051	0.223455865	96.1
6.82377E-09	0.026322939	33	-1.227555743	0.254452956	3.223088924	1.422529813	35.9
6.83526E-09	0.02185311	46	-1.255990055	0.26123279	3.510608204	1.556613615	29.3
6.88001E-09	0.139843747	58	-1.0093959	0.250296208	2.074074074	0.264350529	94.6
6.99125E-09	0.112092321	9	-1.05410803	0.242560421	2.22972973	0.454725487	92.6
7.00522E-09	0.066422391	31	-1.159830873	0.184458943	2.422535211	0.636810415	78.7
7.06315E-09	0.185137758	25	-1.033897579	0.244493514	2.076923077	0.277350098	98.7
7.07613E-09	0.041351063	42	-1.205124201	0.206045411	2.772839506	1.072958843	59.5
7.10128E-09	0.111405219	82	-1.088357797	0.225200353	2.222222222	0.451046427	92.8

bioRxiv preprint doi: https://doi.org/10.1101/863894; this version posted December 4, 2019. The copyright holder for this preprint (which was not certified by peer review) is the author/funder. All rights reserved. No reuse allowed without permission.

7.11413E-09	0.047240915	57	-1.186310723	0.200375135	2.617283951	0.911813098	67.6
7.12264E-09	0.095681196	32	-1.087930411	0.213895125	2.196261682	0.422017891	89.3
7.12753E-09	0.153702421	87	-0.962651569	0.229813026	2.136363636	0.347141757	95.6
7.18259E-09	0.150989175	87	-0.9925314	0.162399352	2.151515152	0.364109541	96.7
7.18950E-09	0.186493724	90	-0.768900939	0.446322541	2.083333333	0.282329851	97.6
7.21488E-09	0.137496908	79	-1.047597322	0.233747406	2.156862745	0.418212818	94.9
7.27193E-09	0.001572966	77	-1.021215784	0.525489134	10.99098196	3.964602509	0.2
7.29832E-09	0.111544153	12	-1.04188503	0.224923369	2.171052632	0.379057002	92.4
7.37434E-09	0.070972038	70	-1.14641744	0.196644062	2.435	0.684189724	80
7.37955E-09	0.179894272	10	-0.921630198	0.373420624	2.235294118	0.562295715	98.3
7.38228E-09	0.077346003	69	-1.105137745	0.209015308	2.307228916	0.609676145	83.4
7.38499E-09	0.074404424	67	-1.147772967	0.214536781	2.45508982	0.691659318	83.3
7.41888E-09	0.184586897	15	-0.988874022	0.225523178	2.136363636	0.351250087	97.8
7.50953E-09	0.138095976	66	-1.034205717	0.212900905	2.127659574	0.396562473	95.3
7.51481E-09	0.026418274	99	-1.250339013	0.251084937	3.350591716	1.45648474	32.4
7.54150E-09	0.077198812	13	-1.157593427	0.195277681	2.46961326	0.792614776	81.9
7.65087E-09	0.084947366	47	-1.108905764	0.203433845	2.298136646	0.510449808	83.9
7.65331E-09	0.032642781	18	-1.222145963	0.254437133	2.985790409	1.193015202	43.7
7.65991E-09	0.025832006	8	-1.265216993	0.25145758	3.418639053	1.568450591	32.4
7.68335E-09	0.010311484	72	-1.333162675	0.312556897	5.847207587	2.559182421	5.1
7.68816E-09	0.079914311	30	-1.137983494	0.206514737	2.38547486	0.637772786	82.1
7.69386E-09	0.188674737	90	-0.989011695	0.209983328	2	0	97.7
7.72114E-09	0.162586604	75	-0.943133758	0.288029914	2.081081081	0.276724731	96.3
7.75176E-09	0.005815423	47	-1.312571945	0.350846263	7.816347124	3.34008032	0.9
7.80529E-09	0.088368467	44	-1.12396216	0.194575843	2.265151515	0.550639441	86.8
7.87197E-09	0.10894672	7	-1.063174882	0.212754079	2.23364486	0.506177671	89.3
7.92871E-09	0.19843264	50	-0.990612648	0.317037141	2.166666667	0.380693494	97.6
7.99685E-09	0.008369269	81	-1.337046159	0.338252918	6.961934156	2.994604067	2.8
8.01327E-09	0.193585215	25	-0.900948362	0.385229867	2.210526316	0.418853908	98.1
8.06551E-09	0.108890271	65	-1.081055455	0.198478403	2.165137615	0.441247421	89.1
8.14365E-09	0.130617238	76	-1.017318034	0.252265869	2.140350877	0.350438322	94.3
8.17114E-09	0.075258332	23	-1.138779245	0.222082313	2.43255814	0.732337485	78.5
8.18483E-09	0.050371983	67	-1.201021438	0.205017868	2.640826873	0.88901607	61.3
8.24470E-09	0.024547216	74	-1.277545786	0.253740075	3.575635877	1.636741586	25.3
8.26690E-09	0.092183487	54	-1.143499769	0.161789778	2.32885906	0.608975136	85.1
8.30507E-09	0.081704416	64	-1.116203165	0.246528133	2.424418605	0.802107756	82.8
8.31030E-09	0.193022601	49	-0.8959442	0.297043347	2.038461538	0.196116135	97.4
8.35460E-09	0.188420479	37	-0.843520223	0.400404285	2.071428571	0.262265264	97.2
8.40694E-09	0.183921943	52	-0.976813403	0.263261996	2.071428571	0.262265264	97.2
8.42181E-09	0.172085151	75	-0.971984654	0.284262444	2.137931034	0.350931203	97.1
8.43248E-09	0.17370966	50	-0.973581436	0.266502793	2.142857143	0.355035801	96.5
8.43370E-09	0.196662612	54	-0.91649985	0.250177244	2.096774194	0.300537154	96.9
8.44681E-09	0.068571065	25	-1.139934404	0.197227753	2.4921875	0.821248153	74.4
8.44749E-09	0.189700816	93	-0.998830845	0.260769879	2.064516129	0.249731038	96.9
8.46323E-09	0.125887308	44	-1.055804236	0.231956951	2.160714286	0.416774878	94.4
8.47772E-09	0.073450666	80	-1.142667633	0.210646128	2.400921659	0.720467363	78.3
8.51053E-09	0.050994876	17	-1.191753039	0.19497868	2.613445378	0.828996046	64.3
8.54517E-09	0.184751248	45	-0.893953272	0.380687338	2.130434783	0.344350222	97.7
8.60084E-09	0.151474097	82	-1.036170237	0.231960913	2.16	0.37032804	95
8.60949E-09	0.10508107	73	-1.092185479	0.227515237	2.290909091	0.564149999	89
8.63334E-09	0.16381068	48	-0.909971561	0.325595286	2.022222222	0.149071198	95.5
8.64179E-09	0.057600032	10	-1.195425726	0.209854215	2.636094675	0.892167775	66.2

bioRxiv preprint doi: https://doi.org/10.1101/863894; this version posted December 4, 2019. The copyright holder for this preprint (which was not certified by peer review) is the author/funder. All rights reserved. No reuse allowed without permission.

8.74248E-09	0.00904102	46	-1.355739991	0.337972087	6.850868233	2.959202271	2.1
8.78851E-09	0.000620664	3	-0.95636245	0.479553828	13.70870871	4.389849176	0.1
8.88195E-09	0.028848465	34	-1.28635734	0.239059698	3.493562232	1.505824903	30.1
8.88317E-09	0.037878753	24	-1.256832911	0.224262038	3.073883162	1.254131228	41.8
8.90884E-09	0.118572492	80	-1.049948124	0.257985408	2.279069767	0.662458217	91.4
8.92040E-09	0.142807314	43	-1.009835488	0.27524197	2.298245614	0.596564937	94.3
8.92560E-09	0.109100561	5	-1.0777045	0.201814829	2.238095238	0.480475955	87.4
8.98107E-09	0.032088454	35	-1.270939853	0.24195228	3.34769688	1.370739574	32.7
8.98286E-09	0.121676149	71	-0.990236976	0.278631082	2.157894737	0.394531488	90.5
8.99266E-09	0.064758017	15	-1.167522903	0.199654594	2.503355705	0.783879338	70.2
2.86874E-09	0.166334062	51	**NA**	**NA**	**NA**	**NA**	100
4.70737E-09	0.108242335	51	**NA**	**NA**	**NA**	**NA**	100
8.12744E-09	0.093878481	55	**NA**	**NA**	**NA**	**NA**	100
2.26321E-09	0.054840814	87	**NA**	**NA**	**NA**	**NA**	100
2.35190E-09	0.164402304	46	**NA**	**NA**	**NA**	**NA**	100
1.27626E-09	0.171937101	95	**NA**	**NA**	**NA**	**NA**	100
3.19730E-09	0.158838896	31	**NA**	**NA**	**NA**	**NA**	100
3.31992E-09	0.072217592	43	**NA**	**NA**	**NA**	**NA**	100
7.12420E-09	0.045272388	13	**NA**	**NA**	**NA**	**NA**	100
8.33616E-09	0.109313414	88	**NA**	**NA**	**NA**	**NA**	100
2.45418E-09	0.18871725	51	**NA**	**NA**	**NA**	**NA**	100
			*__NA__ = Could not be estimated, all replicates were invariable				